Supplemental Information

Supplemental Figure Legends

Supplementary Figure 1. (A-B) Validation of methylation of protein binding microarray using methylation insensitive (MspI) endonuclease. The 40K feature microarray is scanned at 570 nm to detect Cy3-cytosine spiked into the DNA double stranding reactions. Fluorescence intensities before and after methylation were normalized. Probes containing CCGG are in red and remaining features are in black. **(A)** Normalized fluorescence intensities of unmethylated 40K feature microarray before and after MspI digestion. **(B)** Normalized fluorescence intensities of methylated 40K feature microarray before and after MspI digestion. **(C-F)** Effect of protease treatment after methylation on CEBPA-GST and CEBPB-GST binding to the 180K feature microarray. Scatter plot presenting fluorescence intensities **(C-D)** without protease treatment and (**E-F**) with protease treatment after methylation from (**C and E**) CEBPA-GST and (**D and F**) CEBPB-GST. CG-containing 8-mers are in grey; non-CG containing 8-mers are in black. UM: unmethylated array, M: methylated array.

Supplementary Figure 2. Effect of methylation on DNA binding properties of B-ZIP homodimers and heterodimer: (A-C) Z-scores from 40K feature microarray for B-ZIP proteins **(A)** JUN-GST, **(B)** JUND-GST, **(C**) CEBPG-GST. The 8-mers (32,896) are plotted with and without methylation and are color-coded: CG (grey), non-CG (black), TTGC|G (green), CGAT|G (blue) and TGAC|G (red). The best-bound 8-mer is labeled. **(D)** Logos for the 8 B-ZIP homodimers derived from the best-bound unmethylated 8-mers (up to 10) based on Z-scores above 10. **(E)** Hierarchical clustering based on Z-scores obtained from 40K arrays. Replicated experiments cluster together confirming the reproducibility of array results.

Supplementary Figure 3. Effect of methylation on DNA binding properties of 8 B-ZIP homodimers: E-scores from 40K feature microarray for 8 B-ZIP proteins **(A)** CEBPA-GST. **(B**) CEBPG-GST. **(C**) CEBPB-GST. **(D)** CEBPD-GST. **(E**) JUN-GST. **(F)** JUND-GST. **(G**) ATF4-GST. **(H**) CREB1-GST. The figure is based on the same data used in Fig. 1C-H, 2 and SFigure 2A-C**.** The 8-mers (32,896) are plotted with and without methylation and are color-coded: CG (grey), non-CG (black), TTGC|G (green), and TGAC|G (red). The best-bound 8-mer is labeled and logos are derived from the best-bound unmethylated 8-mers (up to 10) based on E-scores above 0.4.

Supplementary Figure 4. Effect of methylation on DNA binding properties of B-ZIP homodimers. Z-scores from 40K feature microarray for B-ZIP proteins **(A)** CEBPA-GST, **(B)** CEBPG-GST, **(C)** CEBPB-GST, **(D)** CEBPD-GST, **(E)** JUN-GST, **(F)** JUND-GST, **(G)** ATF4-GST, **(H)** CREB1-GST. The 5-mers (512) are plotted with and without methylation and are color-coded: CG (grey), non-CG (black). The best-bound 5-mers are labeled. Examination of 5-mer binding identifies that some B-ZIP homodimers bind well to specific half-sites (CEBPB, CEBPD, CREB1) while others show little preference for specific 5-mers (CEBPA, CEBPG, ATF4, and JUN). JUND binds the 5-mer (C|GTGA) that is not part of the best-bound CRE 8-mer.

Supplementary Figure 5. Effect of heterodimerization on the DNA binding properties of CEBPB and ATF4 to unmethylated and methylated 8-mers. (A-C) The 8-mers are color-coded: CG (grey), non-CG (black), TGAC|G (red), TTGC|G (green), and CGAT|G (blue) **(A)** Z-scores from 40K array showing the effect of methylation on binding properties of CEBPB|ATF4-GST. **(B-C)** E-scores from 40K array showing the effect of methylation on the DNA binding properties of the **(B)** CEBPB-GST|ATF4 and **(C)** CEBPB| ATF4-GST heterodimers. Chimeric sequence (TGAC|GCAA) is preferentially bound by both CEBPB-GST|ATF4 **(Fig.1H)** and CEBPB|ATF4-GST when it is unmethylated. The best-bound non-CG 8-mer is TGAT|GCAA, which is the deamination product of the chimeric sequence, TGAC|GCAA. CGAT|GCAA is again the best-bound methylated 8-mer for both CEBPB-GST|ATF4 and CEBPB|ATF4-GST. **(D)** Hierarchical clustering based on Z-scores obtained from 40K arrays for replicated experiments, confirming the reproducibility of array results. **(E-F)** Z-scores for 5-mers from 40K feature microarray for B-ZIP proteins CEBPB-GST|ATF4 **(E)** and CEBPB|ATF4-GST **(F)**. The Z-scores for 5-mers (512) are plotted with and without methylation and are color-coded: CG in grey and non-CG in black, and CGATG in blue. The best-bound 5-mers are indicated by arrows.

Supplementary Figure 6. (A-B) Effect of three different flanking sequences on fluorescence intensities containing CEBP binding sites. In 180K arrays, all non-CG 8-mers (40,545) are presented 2-3 times and all CG containing 8-mers (24,991) are presented three times in different flanking sequences (FS). Fluorescence intensities obtained from the 180K feature array after methylation for **(A)** CEBPA and **(B)** CEBPB binding to CEBP like sequences in three different flanking sequences are shown. **(C-D)** Digestion of **(C)** unmethylated and **(D)** methylated 180K

feature array using methylation insensitive (MspI) endonuclease**.** Fluorescence intensities at 570 nm are plotted for all features, CCGG containing features are colored in red and the remaining features are in black.

Supplementary Figure 7. **(A-B)** Fluorescence intensities of CEBPB-GST binding to the 32,640 8-mers and their respective complementary sequences on **(A)** unmethylated and **(B)** methylated 180K arrays. **(C-D)** Scatter plots comparing Z-scores (40K array) and fluorescence intensities (180K array) for CEBPB-GST binding to (**C**) unmethylated or (**D**) methylated arrays. CG-containing 8-mers are in grey and non-CG containing 8-mers in black. The lack of correlation is attributed to the effect of flanking sequences on the 180K array (T-NNNNNNNN-A).

Supplementary Figure 8. (A-B) The effect of methylation on DNA binding properties of CEBPB|ATF4 heterodimer. Fluorescence intensities at 660 nm from the 180K feature microarray are plotted for all of the 65,536 8-mers in the background T-NNNNNNNN-A. Lines are fitted to the 64 8-mers containing the color coded 5-mers and non-CG 8-mers as described in **Fig. 3**. **(A)** Effect of methylation on DNA binding of CEBPB|ATF4-GST. **(B)** Effect of methylation on DNA binding when both monomers are labeled with GST (CEBPB-GST|ATF4-GST). Similar results are obtained as in Fig. 3E. **(C)** EMSA using purified CEBPB, ATF4, and CEBPB|ATF4 B-ZIP domain dimers mixed with unmethylated and methylated CGAT|GCAA containing DNA probes. Protein dimer concentrations are indicated. * indicates protein-DNA complexes at the lowest protein concentration. Note that the CEBPB|ATF4-DNA complex moves slower than CEBPB-DNA complex, and faster than ATF4-DNA complex. **(D)** EMSA using *in vitro* translated CEBPB-GST|ATF4 B-ZIP proteins mixed with unmethylated, two hemimethylated and methylated CGAT|GCAA containing DNA probes (lanes 1-20). Last two lanes are the EMSA using *in vitro* translated CEBPB-GST with unmethylated and methylated CGAT|GCAA containing DNA probes.

Supplementary Figure 9. (**A)** EMSA showing CEBPB|ATF4 heterodimer preferentially binds to unmethylated TTGC|GTCA. Purified CEBPB, ATF4, and CEBPB|ATF4 B-ZIP domain dimers were mixed with unmethylated, hemi-methylated or methylated TTGC|GTCA containing DNA probes. Protein dimer concentrations are indicated. Asterisks mark lanes with the same protein concentration. **(B)** EMSA showing CEBPB preferentially binds to methylated ATTGC|GCAAT without Mg^{2+} in the gel or in the binding reactions. Purified CEBPB B-ZIP

domain dimers were mixed with methylated or unmethylated DNA probes containing the same consensus TTGC|GCAA 8-mer but different flanking nucleotides at the 5´ and 3´ end of the 8-mer. Protein dimer concentrations are indicated. No Mg^{2+} in the gel or in the binding reactions.

Supplementary Figure 10. (A) Distribution of CG methylation status in primary female mouse dermal fibroblasts. **(B)** Percent of CGs with increasing read depth (red is forward strand and blue is reverse strand). More than 90% of the total cytosine's in the CG have read depth >10X.

Supplementary Figure 11. (A) Number of CEBPB ChIP-seq peaks before and after thapsigargin treatment and ATF4 ChIP-seq peaks after thapsigargin treatment **(B)** Percentage of all 8-mers in CEBPB ChIP-seq peaks in the mouse dermal fibroblasts plotted against CEBPB-GST binding using $\log_{10}$ Z-scores for methylated array. **(C-F)** Methylation status of canonical CEBP sites (TTGC|GCAA) in **(C)** the whole genome and **(D)** CEBPB ChIP-seq peaks of mouse dermal fibroblasts. **(E-F)** Methylation status of canonical CREB1 sites (TGAC|GTCA) in **(E)** whole genome, and **(F)** CREB1 ChIP-seq peaks of mouse dermal fibroblasts.

Supplementary Figure 12. (A-B) Percent of all 8-mers in CEBPB ChIP-seq peaks in mouse dermal fibroblasts after ATF4 induction by thapsigargin plotted against CEBPB-GST|ATF4 heterodimer binding using **(A)** Z-scores and **(B)** $\log_{10}$ Z-scores for methylated arrays. **(C)** Enrichment of 8-mers in CEBPB ChIP-seq peaks before and after treatment with thapsigargin. (**D**) Enrichment of 8-mers in CEBPB and ATF4 ChIP-seq peaks after treatment with thapsigargin.

Supplementary Figure 13. (A-B) Changes in CEBPB binding to methylated 8-mers 1 CG dinucleotide after ATF4 induction vs. **(A)** Z-score and **(B)** $\log_{10}$ Z-scores for CEBPB-GST|ATF4 heterodimer binding to 8-mers from methylated arrays. **(C-D)** Enrichment of 8-mers with 1 CG dinucleotide in CEBPB ChIP-seq peaks before and after treatment with thapsigargin in linear (**C**) and logarithmic (**D**) scale. (**E-F**) Enrichment of 8-mers with 1 CG dinucleotide in CEBPB and ATF4 ChIP-seq peaks after treatment with thapsigargin in linear (**E**) and logarithmic (**F**) scale.

Supplemental Tables

Supplementary Table 1. (A-B) Estimation of length of CEBP motif from 40K **(A)** and 180K **(B)** array. Z-scores obtained from 40K array for CEBP site, TGC|GCAAN to identify the potential 9-mer sequence by extending to the 3′ side of the 8-mer. For all CEBP family members (CEBPA, CEBPB, CEBPG and CEBPD), the highest values of Z-scores are for 8-mer with "T" on 3′ side (TGCGCAAT). Further extension to the 3′ side, GC|GCAATN lead to considerable decrease in Z-score values for all the CEBP family members as well as no preferred binding for any specific nucleotide. Since the Z-score values for the complementary sequences are same we can extend the 8-mer NTTGC|GCA to the 5′ side, the most preferred sequence will be the palindromic 10-mer ATTGC|GCAAT. **(C)** Estimation of length of TRE and CRE motifs. Z-scores obtained from 40K array for TRE-N (TGAGTCAN and TGACTCAN) and CRE-N (GAC|GTCAN) to identify the potential 9-mer sequences by extending to the 3′ side of the 8-mer. For JUND and JUN highest values for Z-scores are obtained for TRE 8-mer with a "T" on 3′ side TGA[G/C]TCAT. Extending to the 3′ side for CRE site, GAC|GTCAN "A" on 3′ is least preferred by CREB1 suggesting the site to be GAC|GTCAB, where B= C, G or T. (D) P-values (40K and 180K arrays)

Supplementary Table 2. Z-score from 40K array for homodimers (CEBPB and ATF4) and heterodimers (CEBPB-GST|ATF4 and CEBPB|ATF4-GST) for canonical CEBP, canonical CRE, chimera and CGATG site. Binding of CEBPB to the canonical CEBP site (TTGC|GCAA) is enhanced by methylation. However, methylation decreases binding of ATF4 to the best bound canonical CRE site (TGAC|GTCA). Similarly methylation also decreases binding of heterodimers (CEBPB-GST|ATF4 and CEBPB|ATF4-GST) to the chimeric site TGAC|GCAA. However, methylation considerably potentiates binding of heterodimers to CGATG site (CGAT|GCAA).

Supplementary Table 3. (A) Ratio of fluorescence intensities for the best versus the worst bound 8-mer sequences by CEBPB or ATF4 homodimers and ATF4|CEBPB heterodimer on180K array. **(B)** Fluorescence intensities (×1,000) from 180K array for homodimers (CEBPB and ATF4) and heterodimers (CEBPB-GST|ATF4 and ATF4-GST|CEBPB) for canonical CEBP, CRE, chimera and CGAT|G: Binding of CEBPB to the canonical CEBP site (ATTGC|GCA*A*) is enhanced by methylation. *A* (italics) is from the flanking array sequence that is part of the

binding site. However, methylation decreases binding of ATF4 to the best bound canonical CRE site (ATGAC|GTC*A*). Similarly methylation also decreases binding of heterodimers (CEBPB-GST|ATF4 and ATF4-GST|CEBPB) binding to the chimeric site CTGAC|GCA*A*. However, methylation considerably potentiates binding of heterodimers to CGAT|G site (CCGAT|GCA*A*) as observed in 40K array. **(C)** Methylated 8-mer NCGAT|GCA*A* bound well by ATF4|CEBPB heterodimer. Fluorescence intensities (×1,000) obtained from 180K array for homodimers (CEBPB and ATF4) and heterodimer (CEBPB|ATF4) binding to NCGAT|GCA*A* for the identification of the potential 9-mer sequence by extending to the 5´ side of 8-mer. *A* (italics) is from the flanking array sequence that is part of the binding site. "T" on the 5´ side of "TCGAT|GCA*A*" is not preferred by heterodimers CEBPB|ATF4 after methylation**.**

Supplementary Table 4. (A) Genome wide cytosine methylation in the context of CG, CHG and CHH (H=A, C, T) in mouse primary dermal fibroblasts with a coverage of 50X. **(B)** Occurrences of CEBP 10-mer, 8-mer, deaminated 8-mer, CGAT|GCA and deaminated chimeric CEBP-CRE motifs in the genome, number with a known methylation status in dermal fibroblasts, and fraction of unmethylated and methylated motifs bound by CEBPB before and after ATF4 induction in the unmasked genome. **(C)** CREB1 binding to unmethylated and methylated CRE 8-mers (TGAC|GTCA) in female mouse primary dermal fibroblasts

Supplementary Table 5. (A) *In vivo* and *in vitro* CEBPB binding to unmethylated and methylated CEBP like 9-mers. **(B)** CEBPB binding to unmethylated and methylated CEBP like 10-mers in mouse primary dermal fibroblasts.

Supplementary Table 6. (A) Enriched GO Terms for genes bound by CEBPB in dermal fibroblasts with TGAT|GCAA motif within -10kbp to 1kbp of the TSS after ATF4 induction by *Tg*. **(B)** P-values based on fraction of CEBP ChIP-seq peaks vs non peaks containing K-mers with mCGAT|G before and after ATF4 induction. **(C)** Enriched GO Terms for genes bound by CEBPB in dermal fibroblasts with methylated and unmethylated CGAT|G motif within -10kbp to 1kbp of the TSS after ATF4 induction by *Tg*.

Supplementary Table 7. B-ZIP domain sequences used in this study.

Supplementary Figure 1:

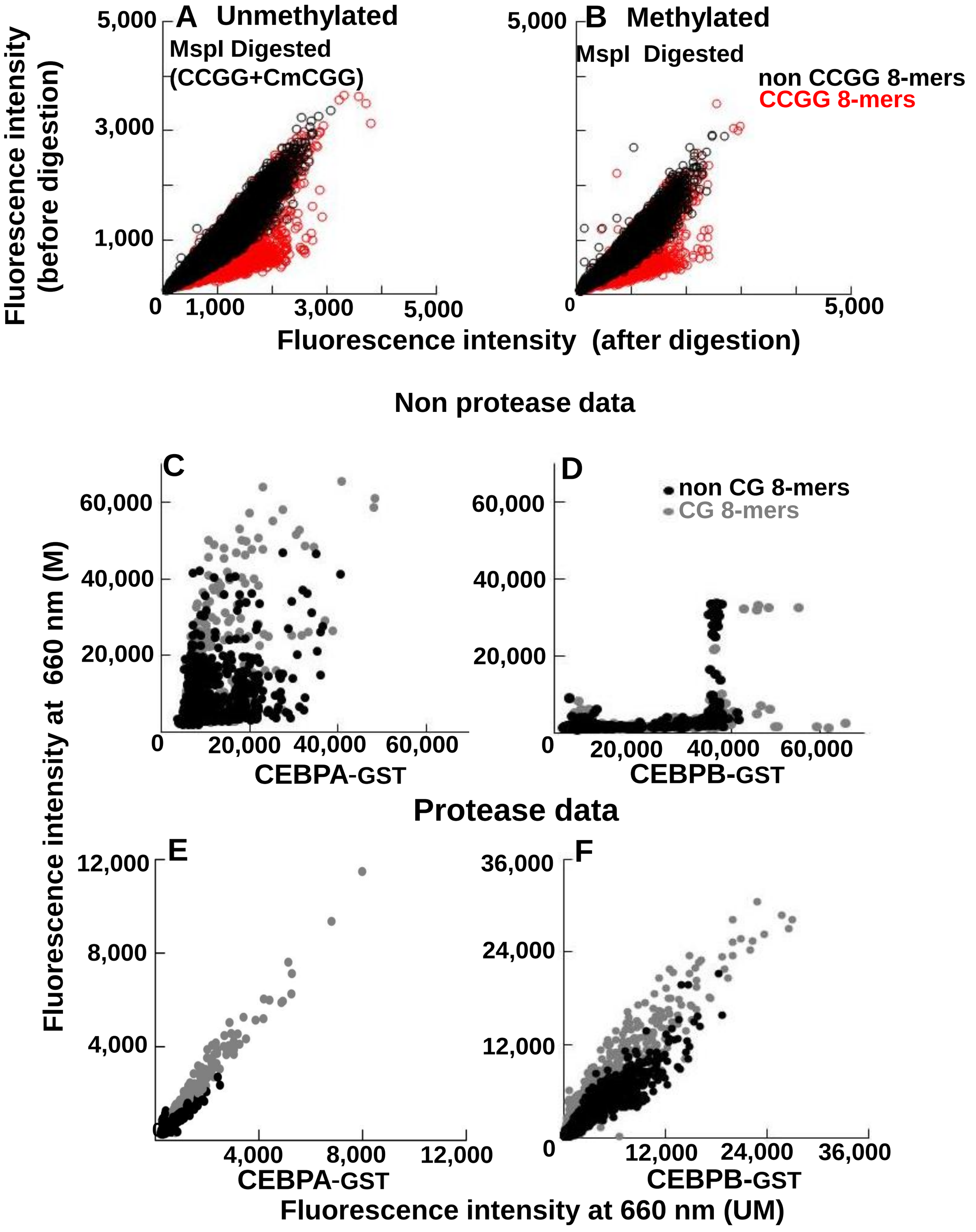

Supplementary Figure 2:

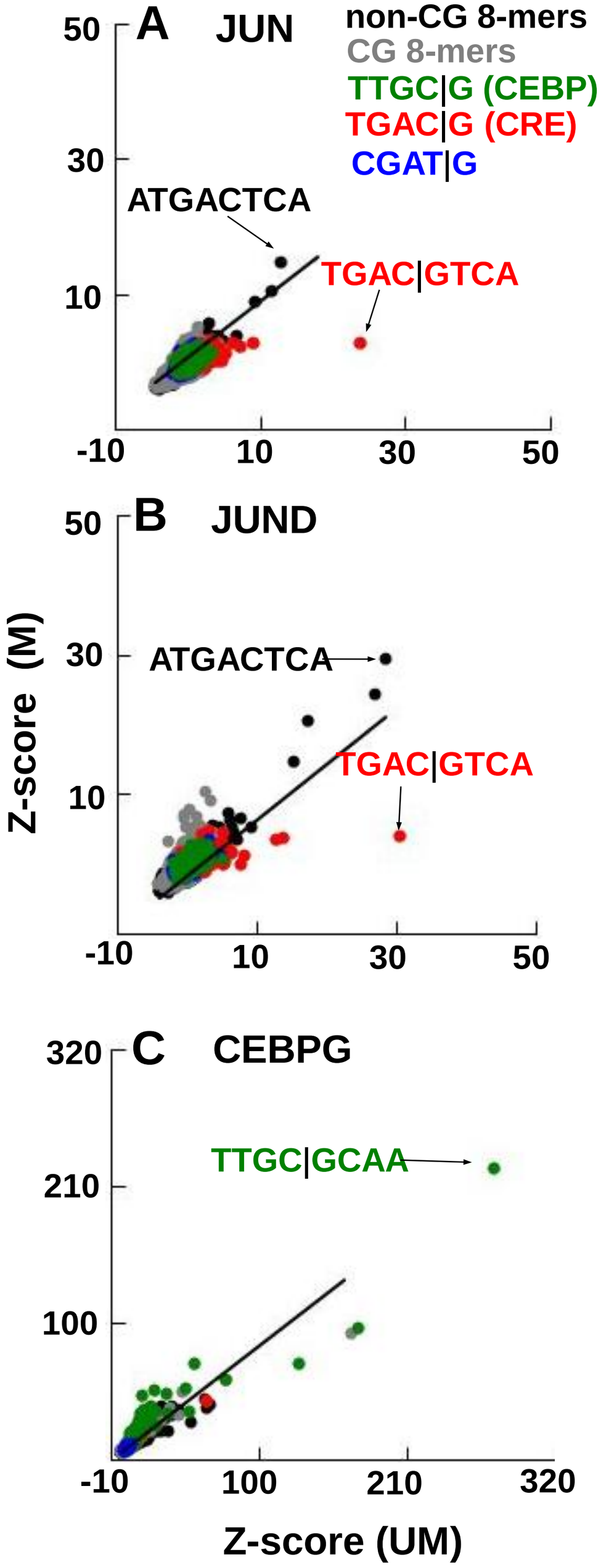

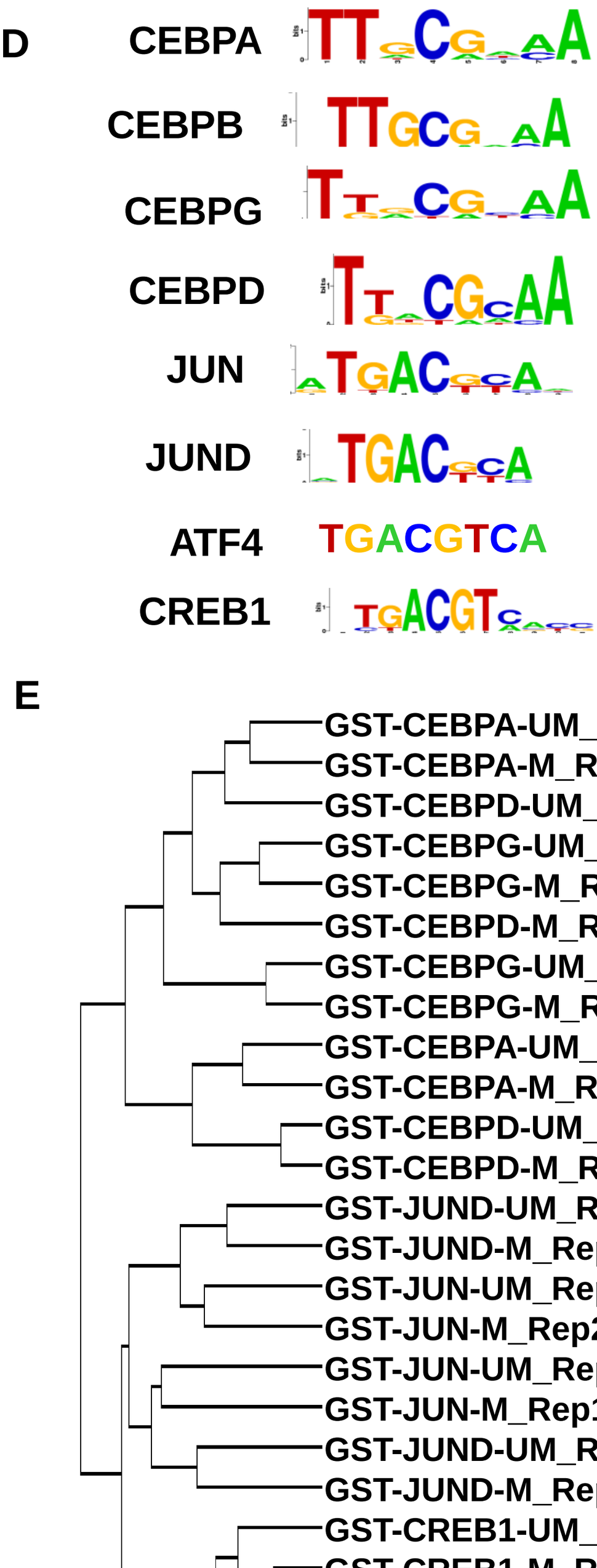

Supplementary Figure 3:

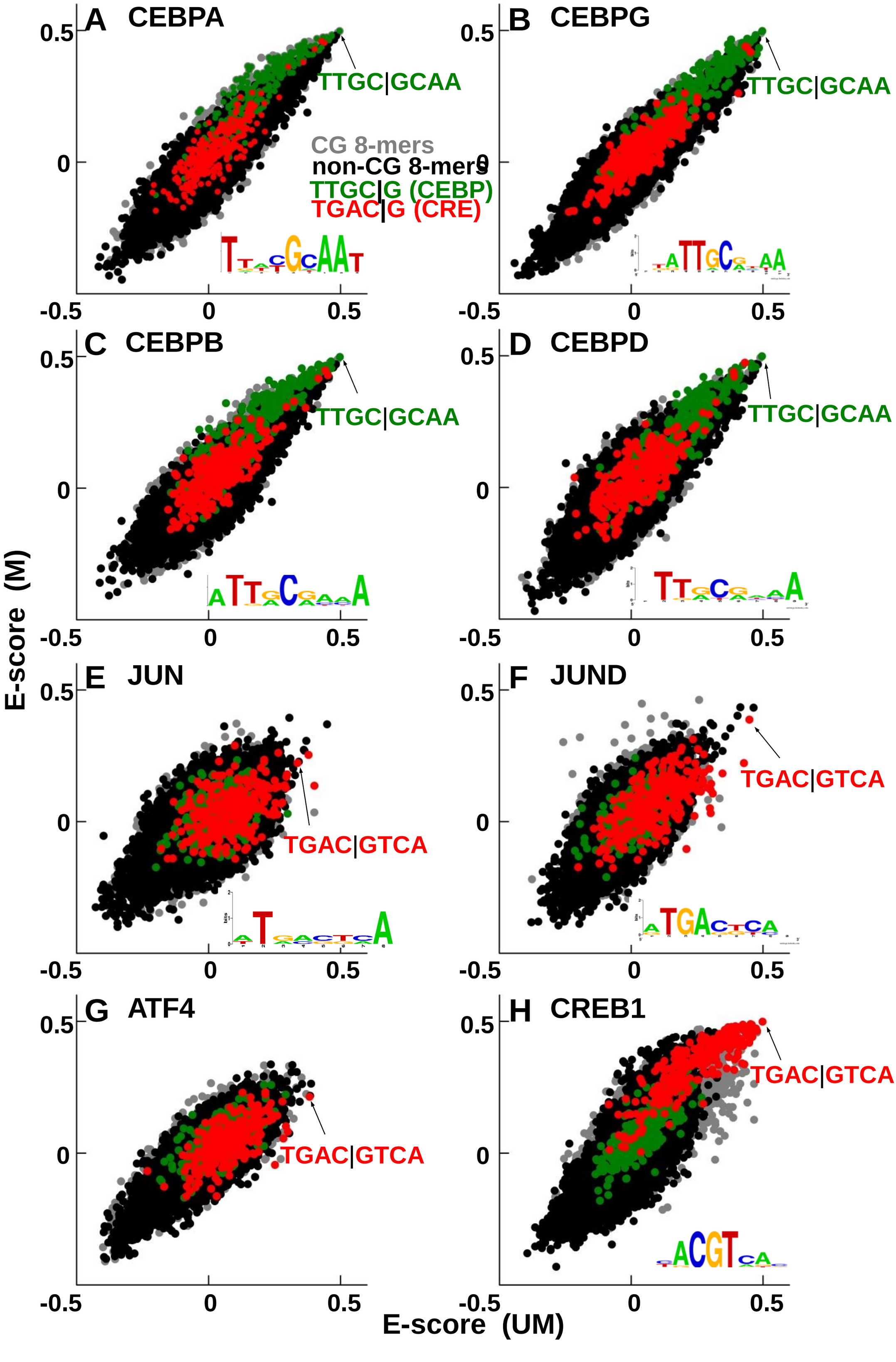

Supplementary Figure 4:

Supplementary Figure 5:

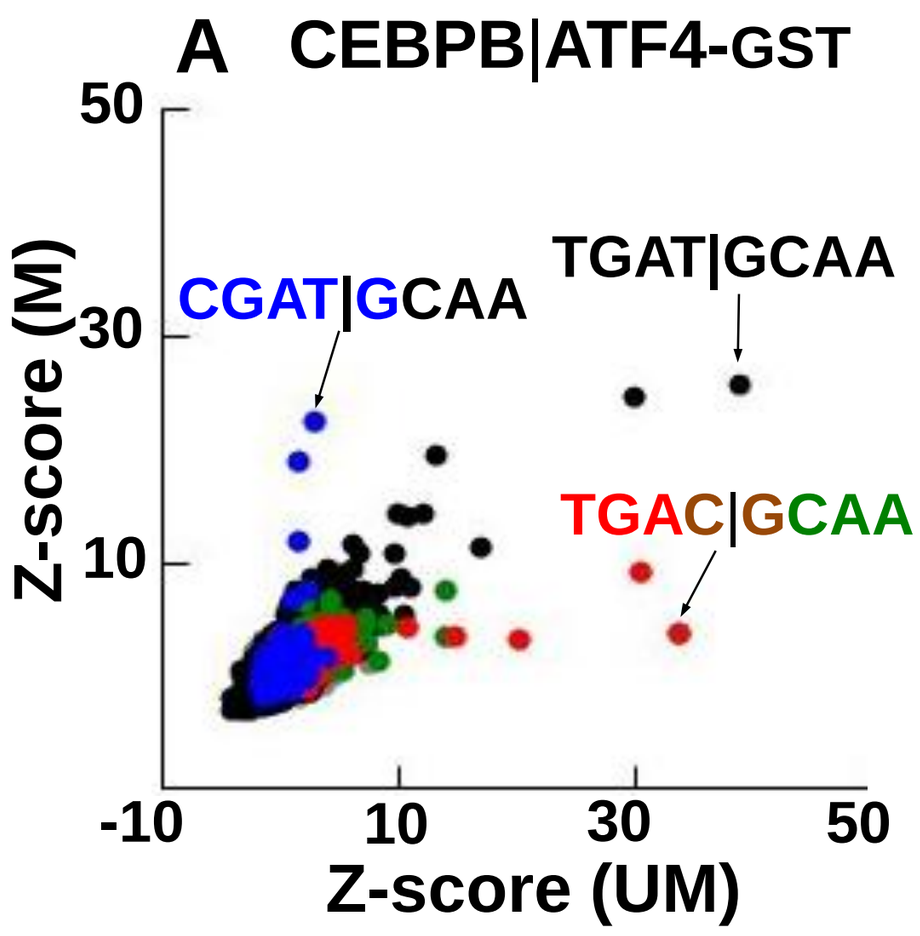

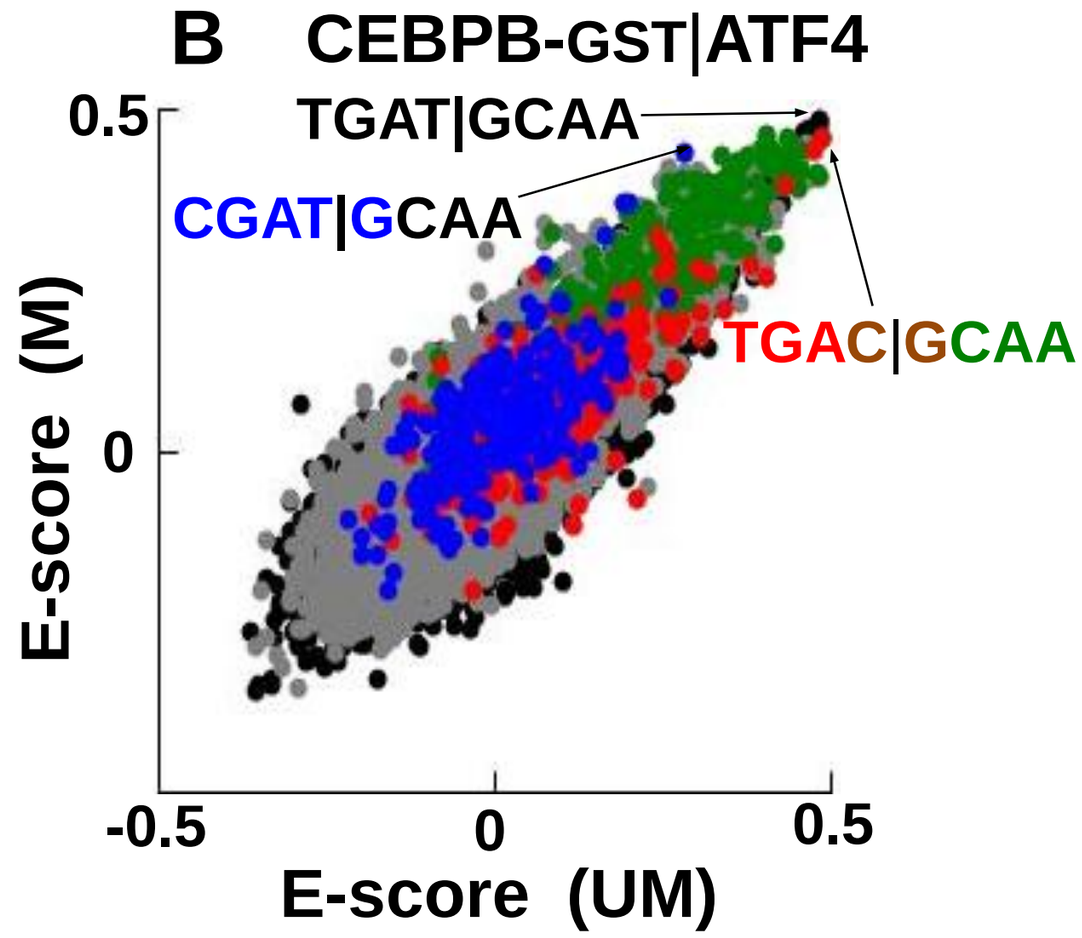

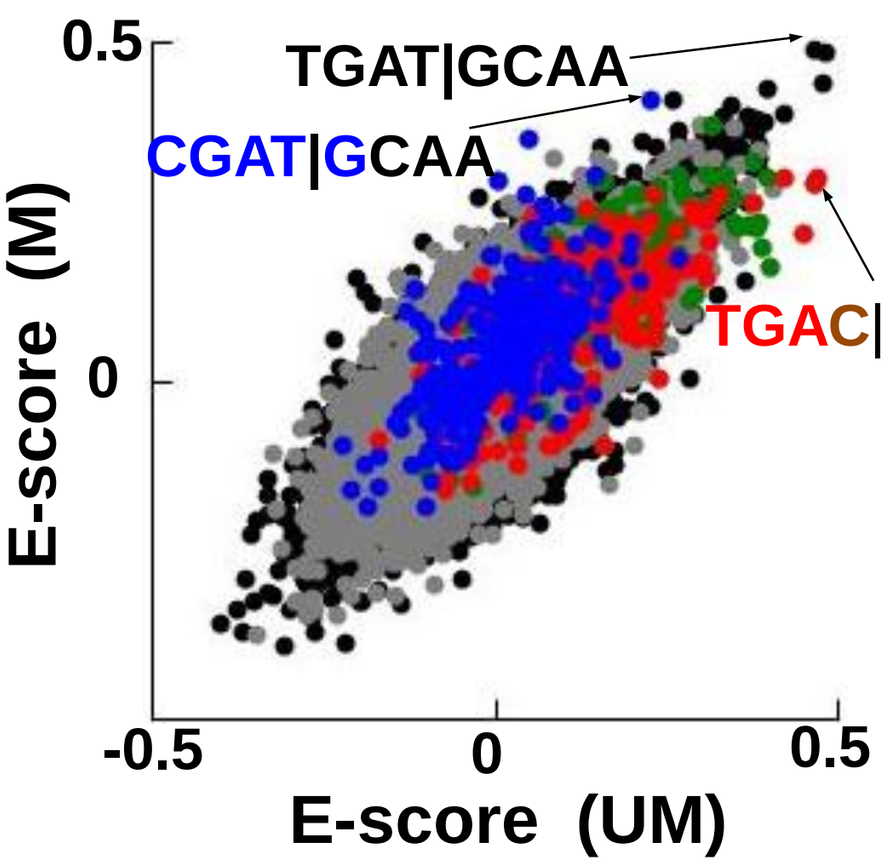

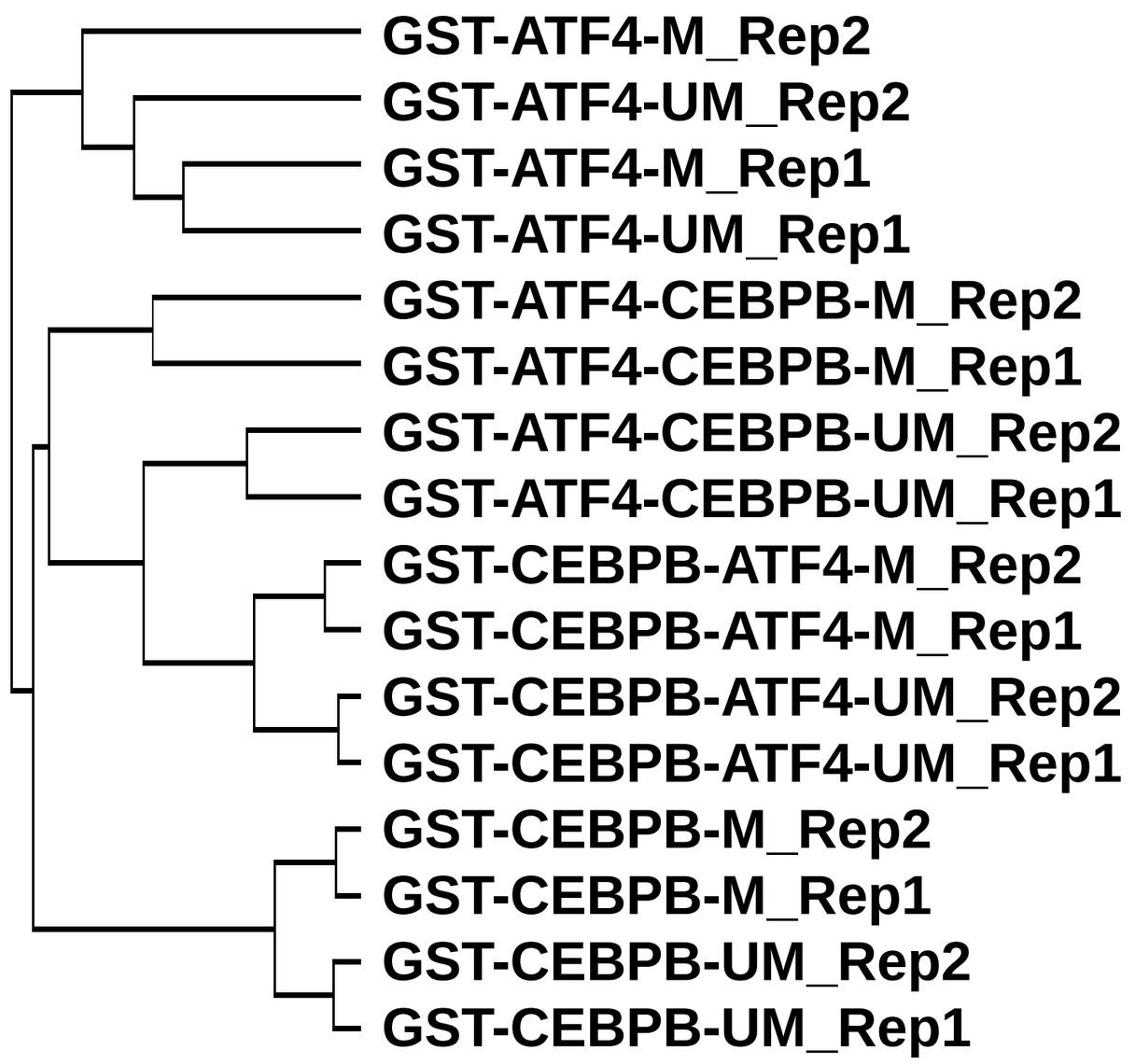

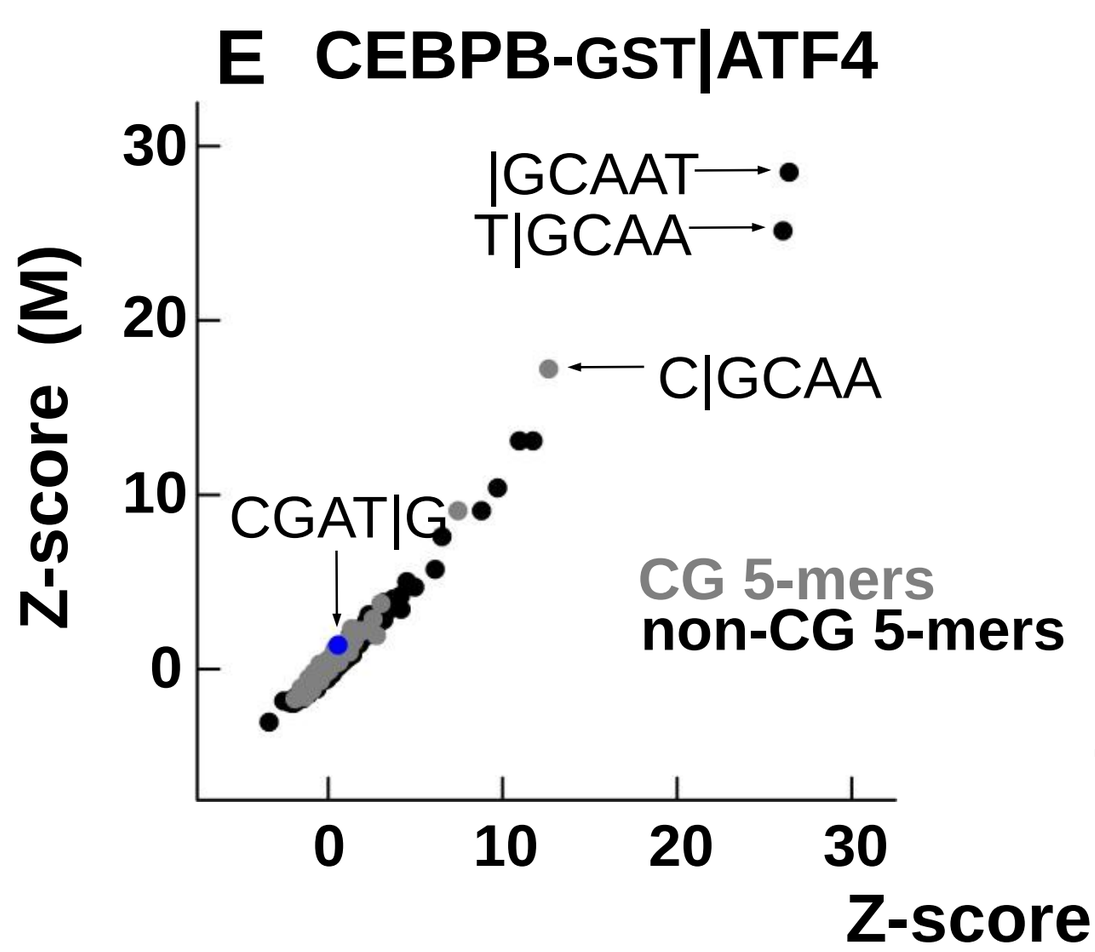

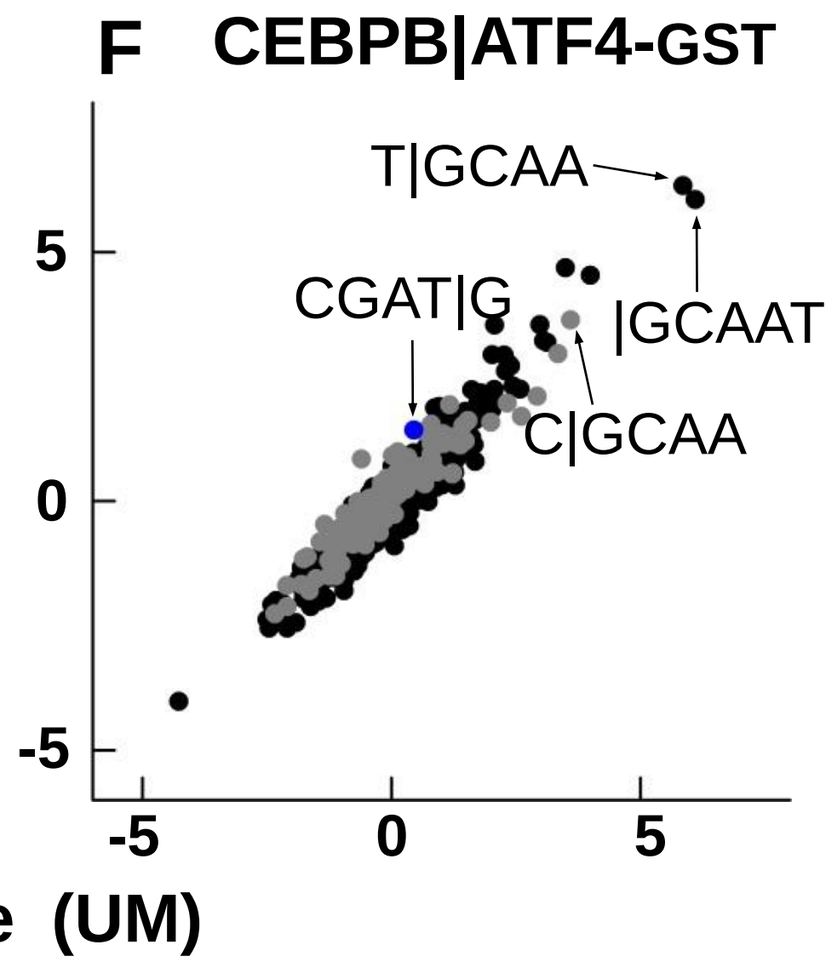

Supplementary Figure 6:

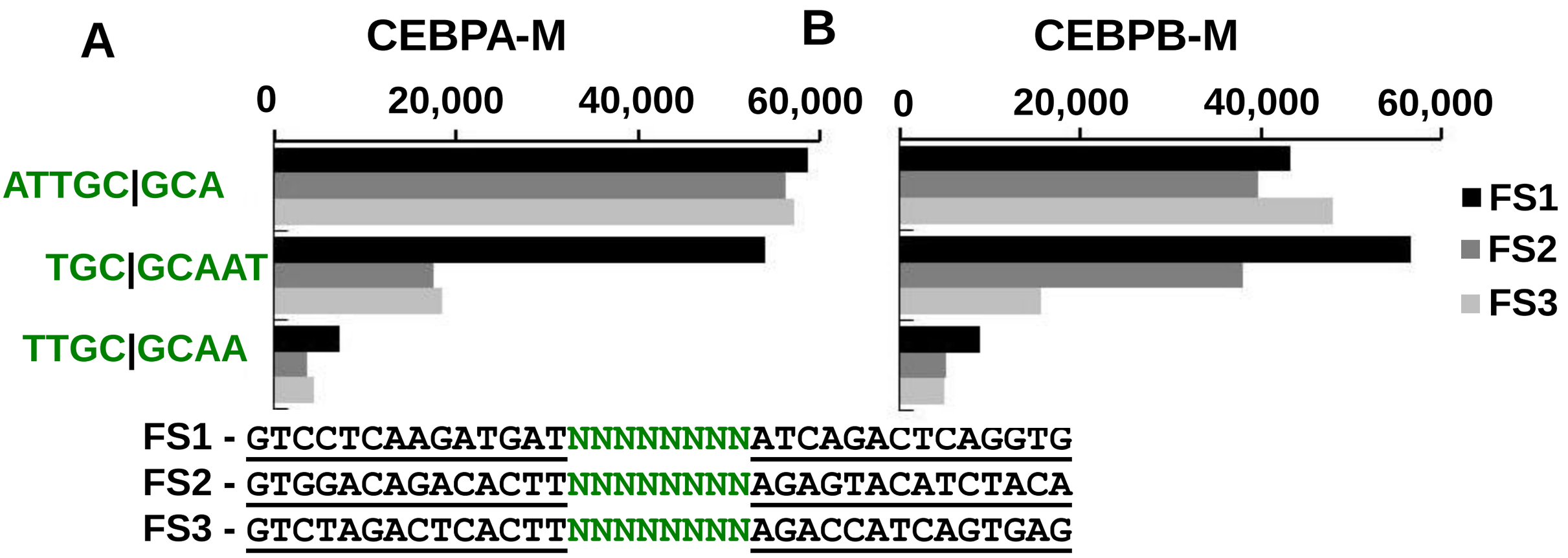

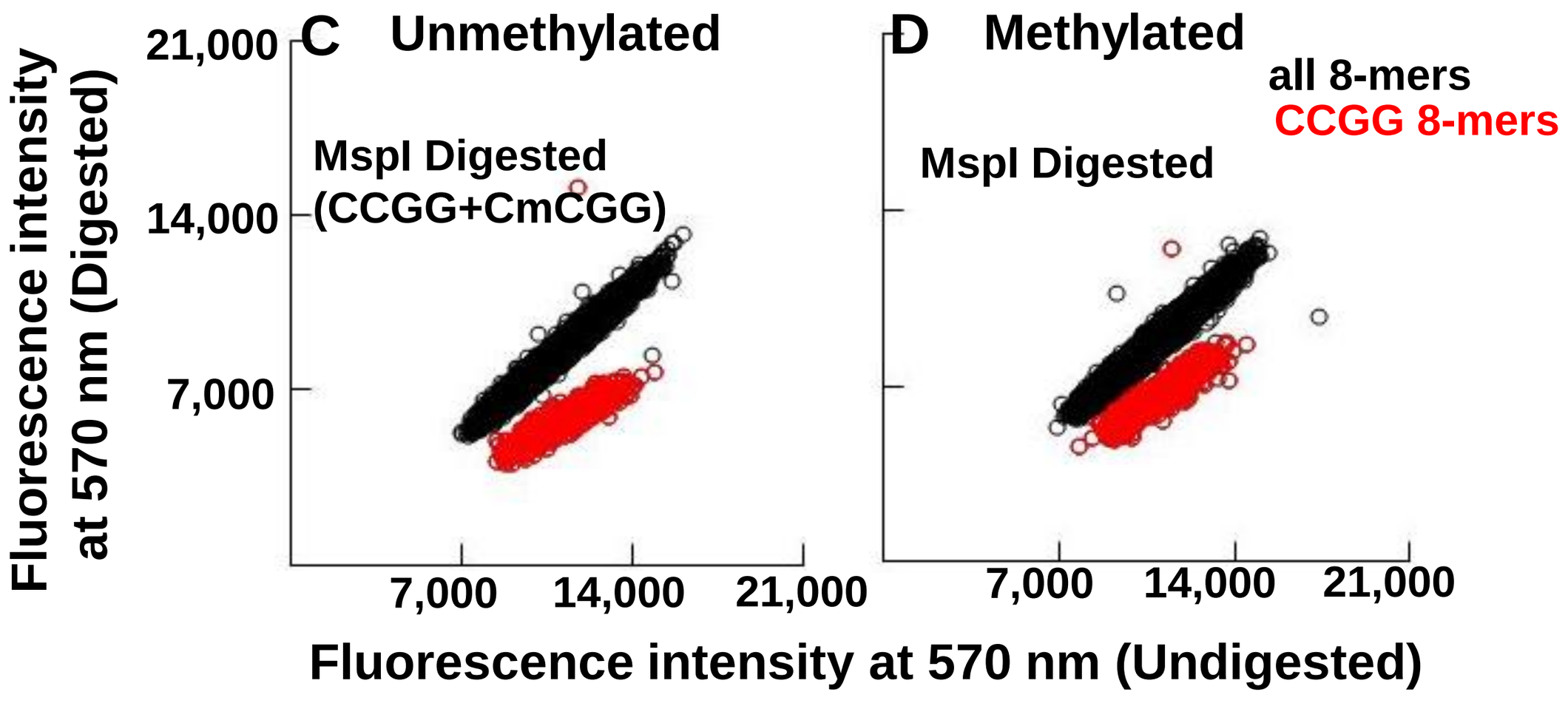

Supplementary Figure 7:

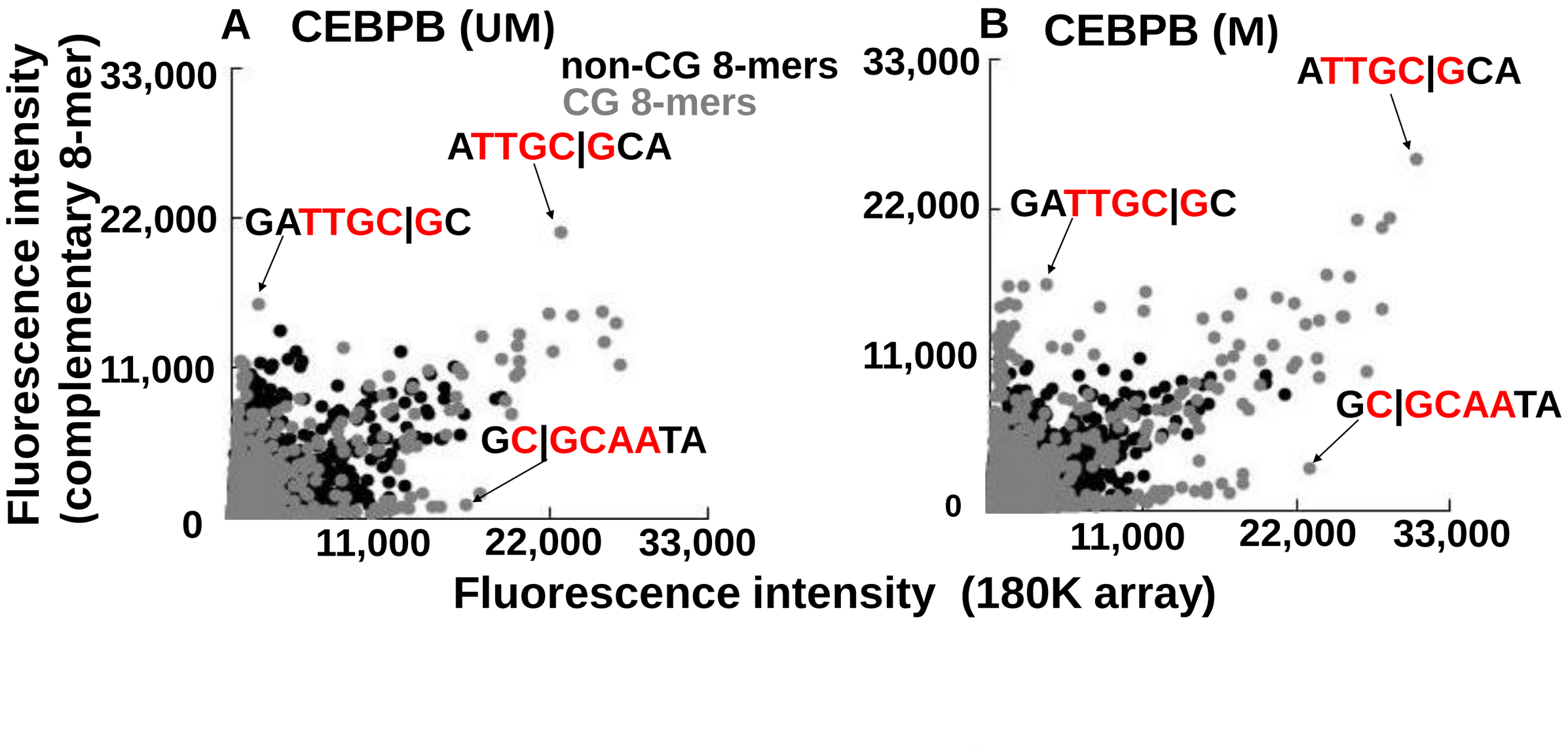

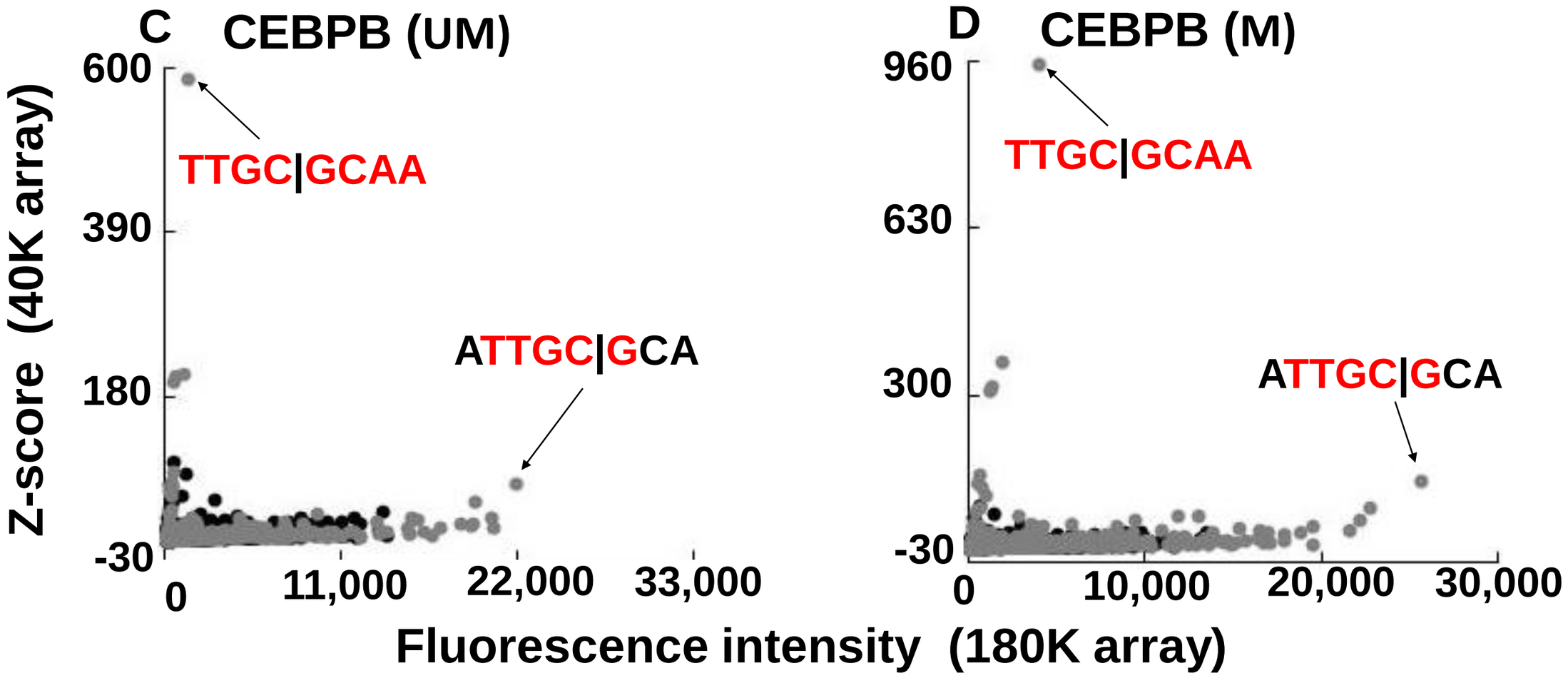

Supplementary Figure 8:

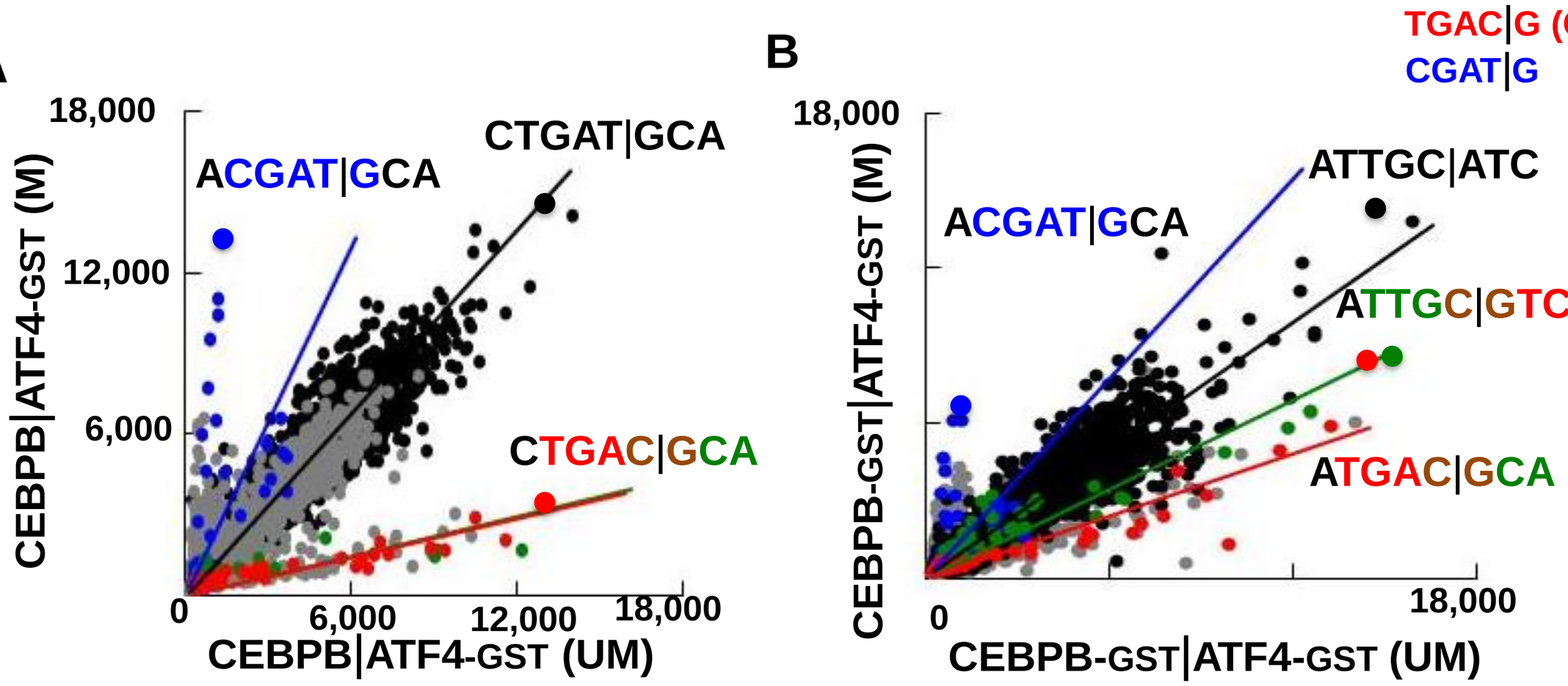

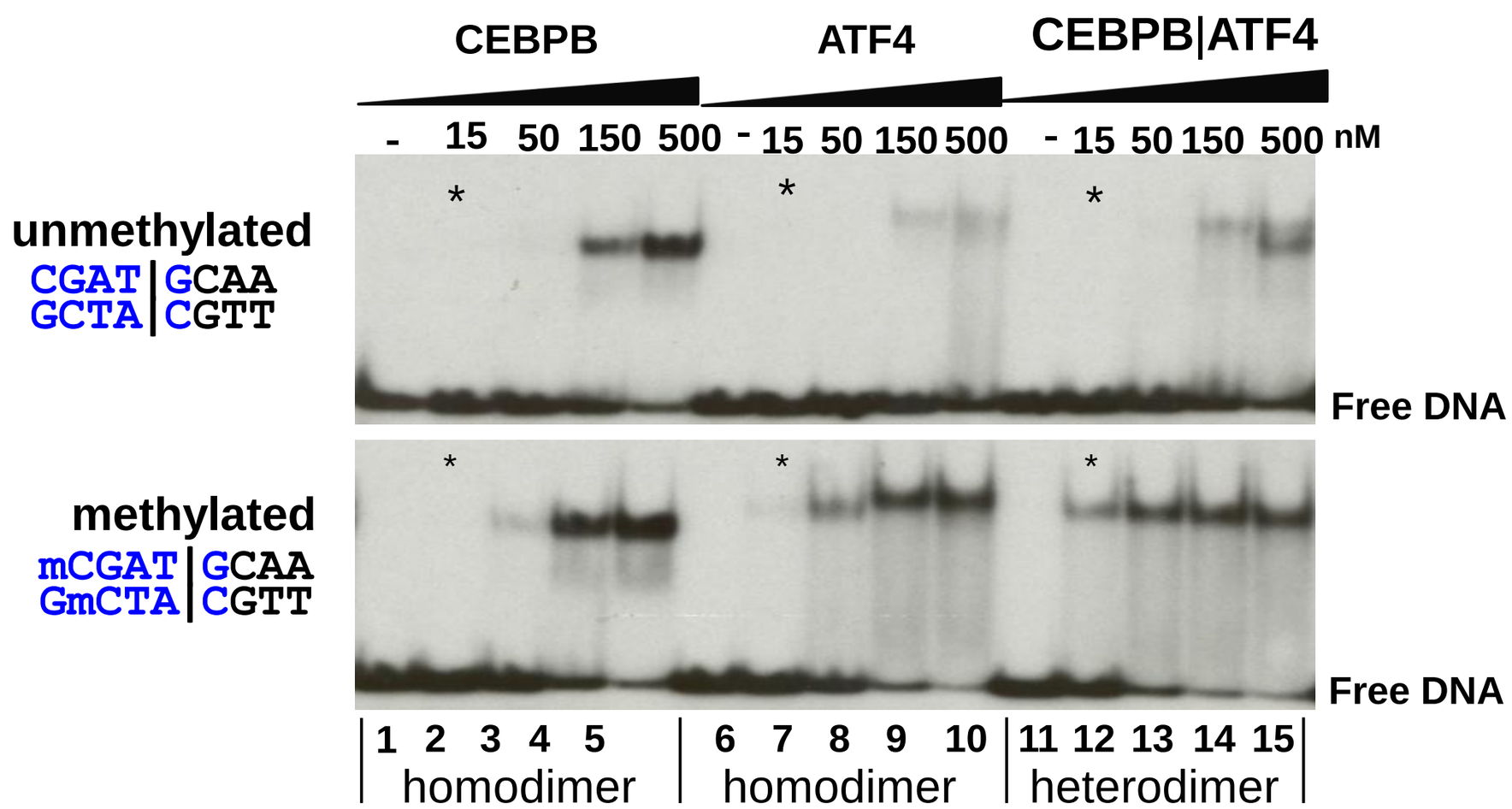

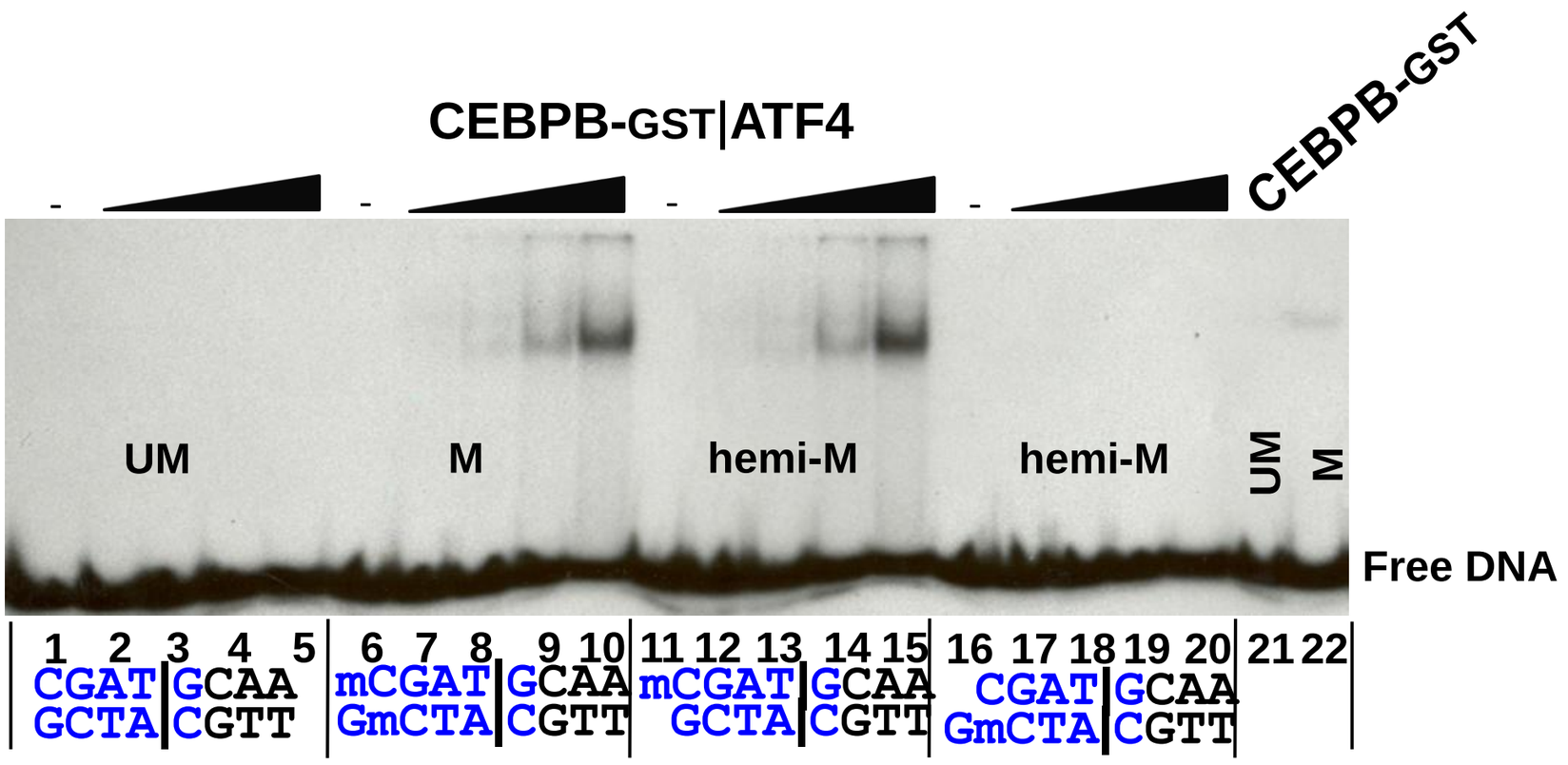

Supplementary Figure 9:

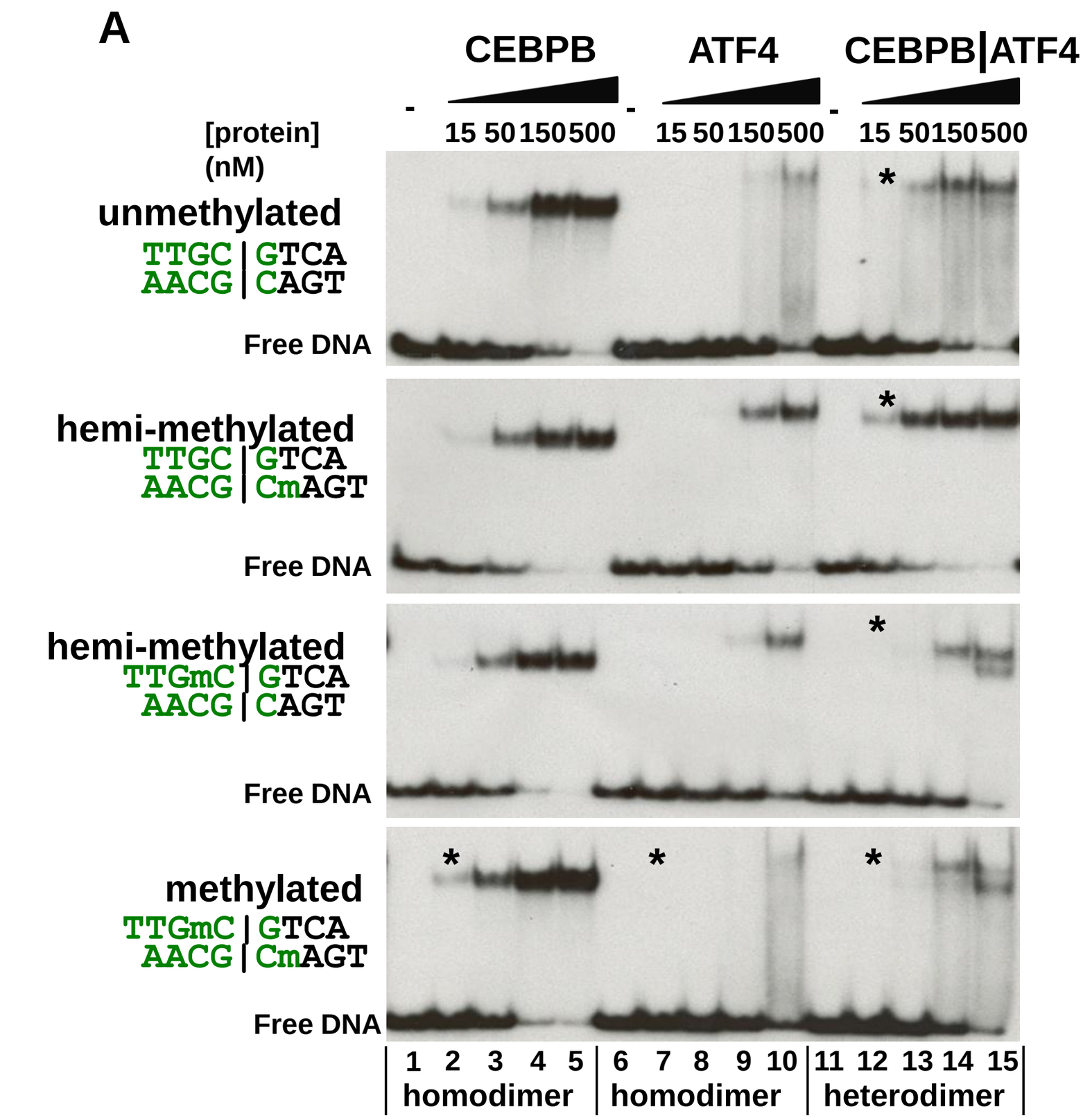

Supplementary Figure 10:

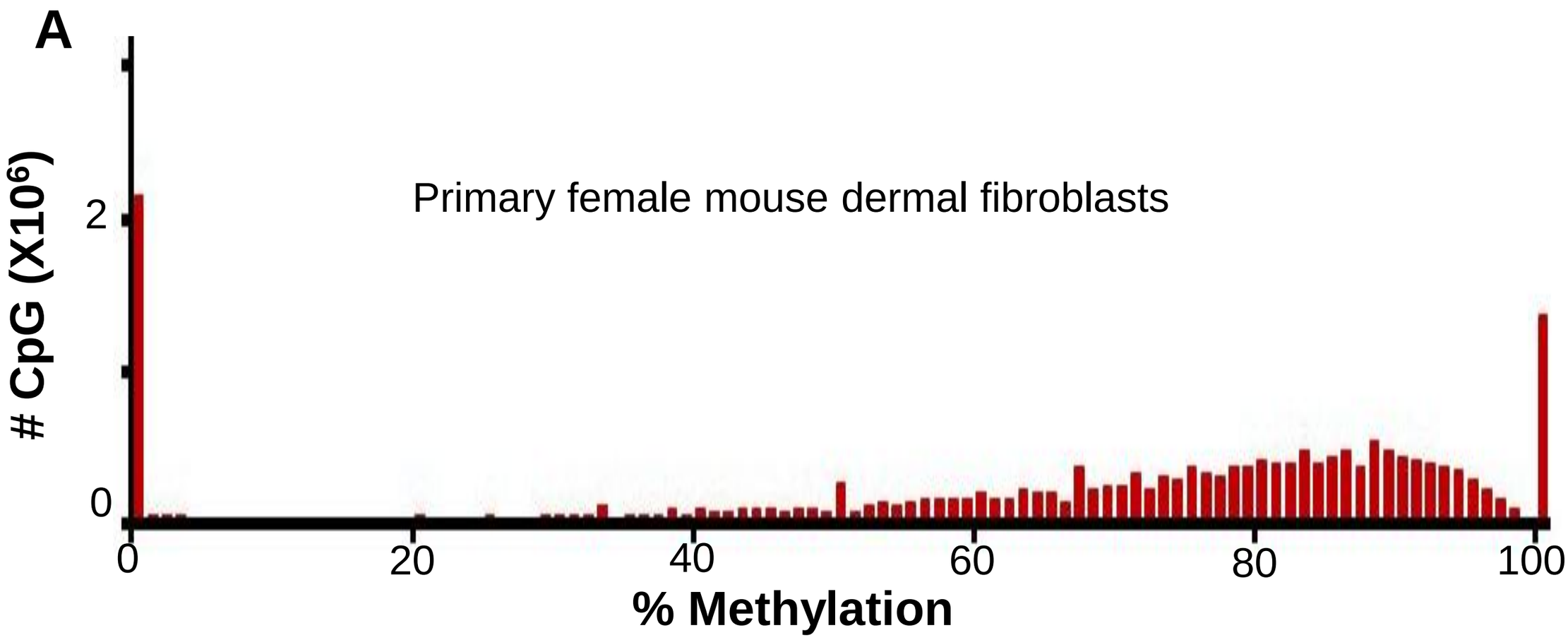

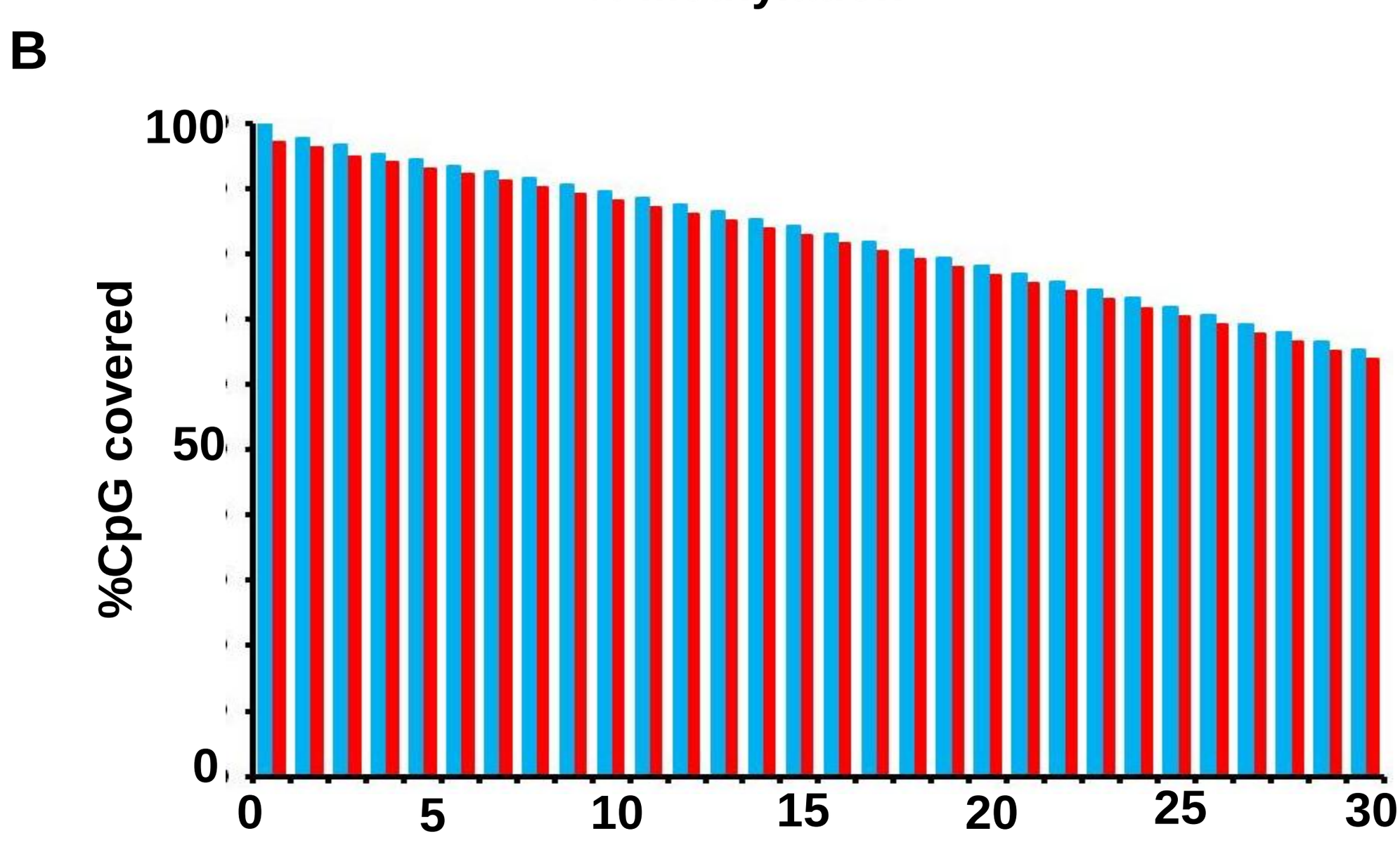

Supplementary Figure 11:

A

CEBPB, ATF4 ChIP-seq reads

	CEBPB before Tg treatment	CEBPB after Tg treatment	ATF4 after Tg treatment
Total Reads	30,086,290	17,869,736	13,204,536
Reads after duplicate removed	26,668,039	11,539,064	11,233,064

B

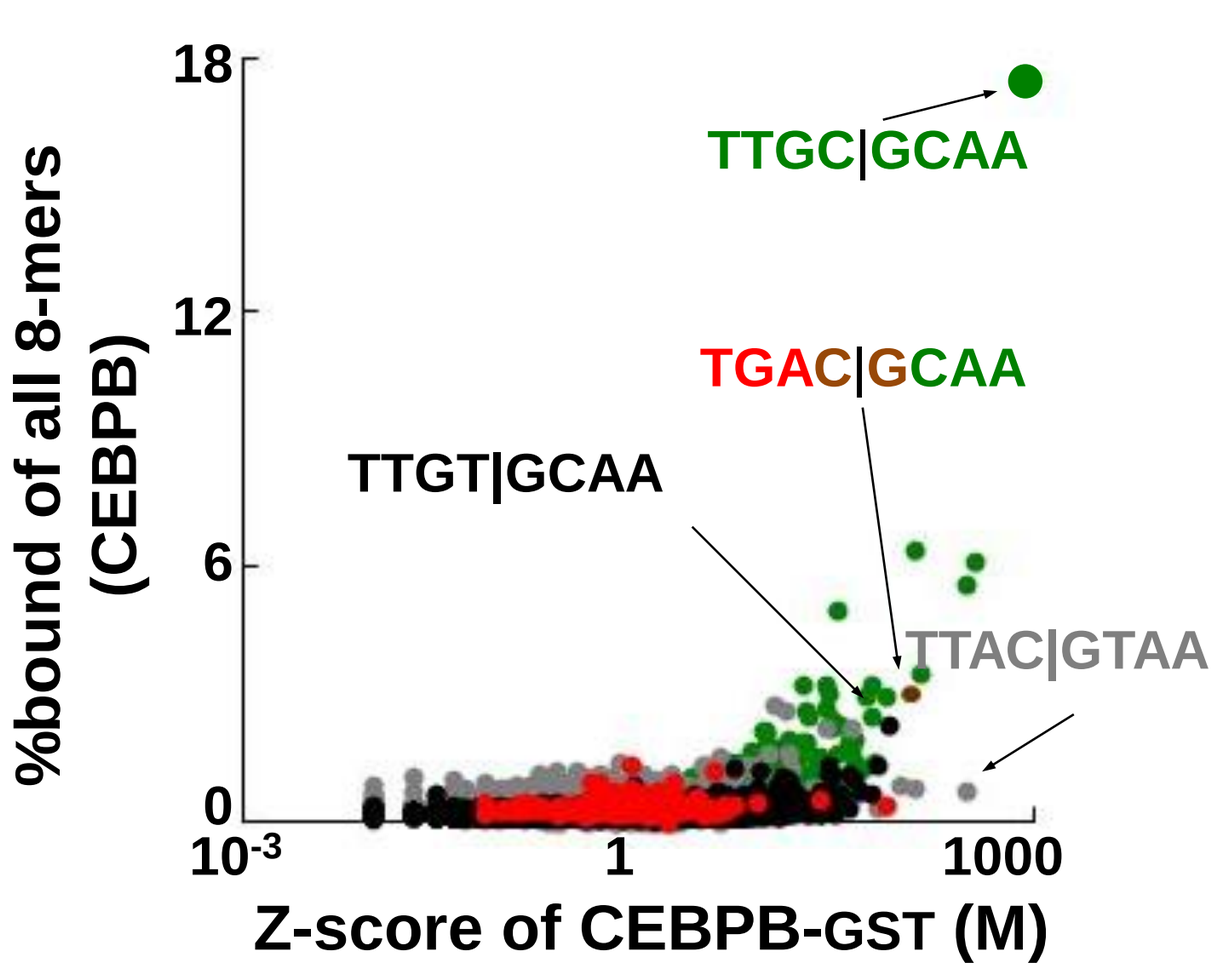

TTGCGCAA (Consensus site: 306 bound by CEBPB ChIP-seq and 187 >50% methylated & 119 <50% methylated)

C

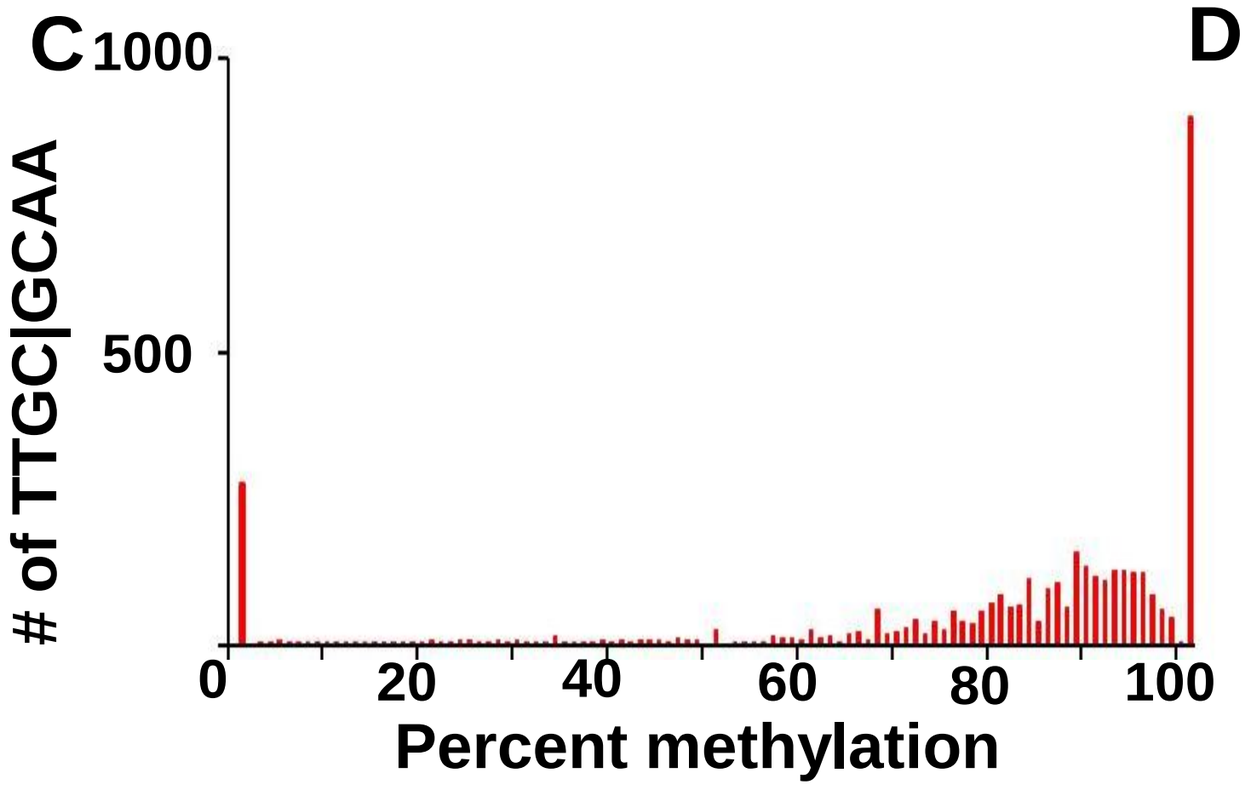

D

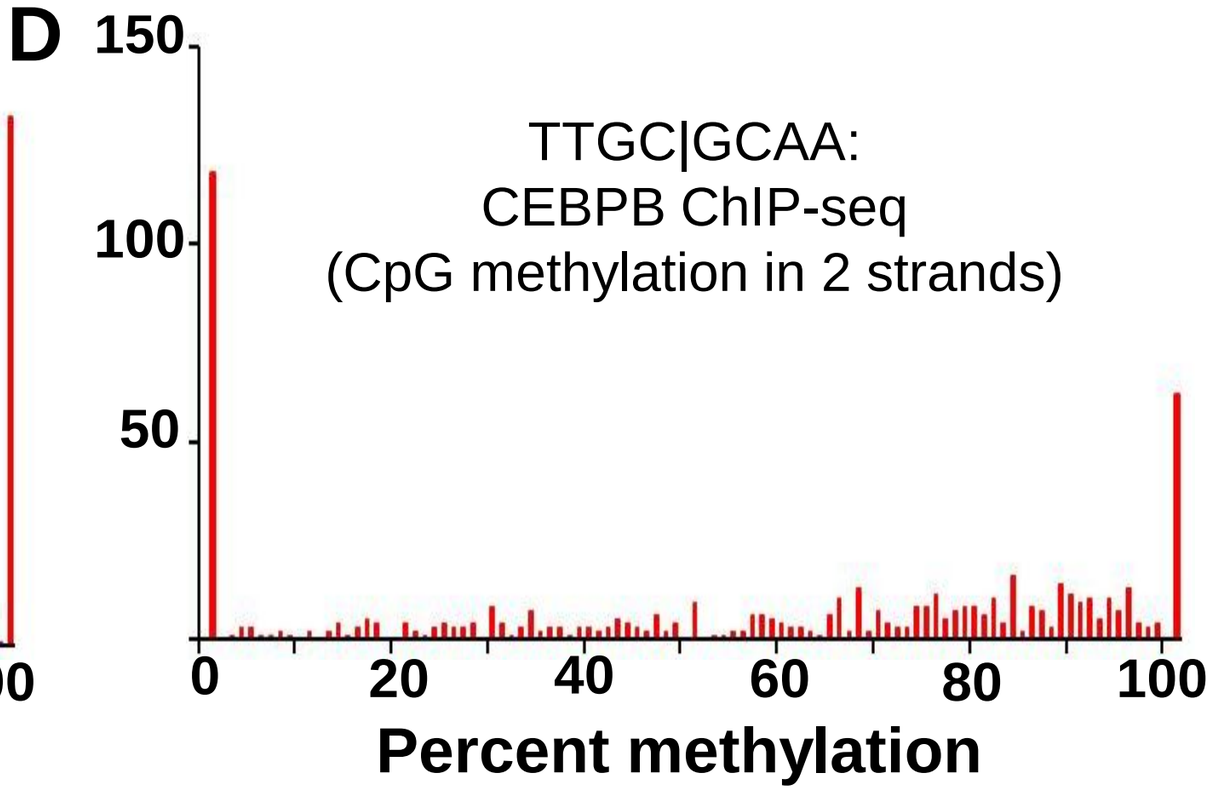

TGAC|GTCA (Consensus site: 141 bound by CREB1 ChIP-seq and all of them are unmethylated)

E

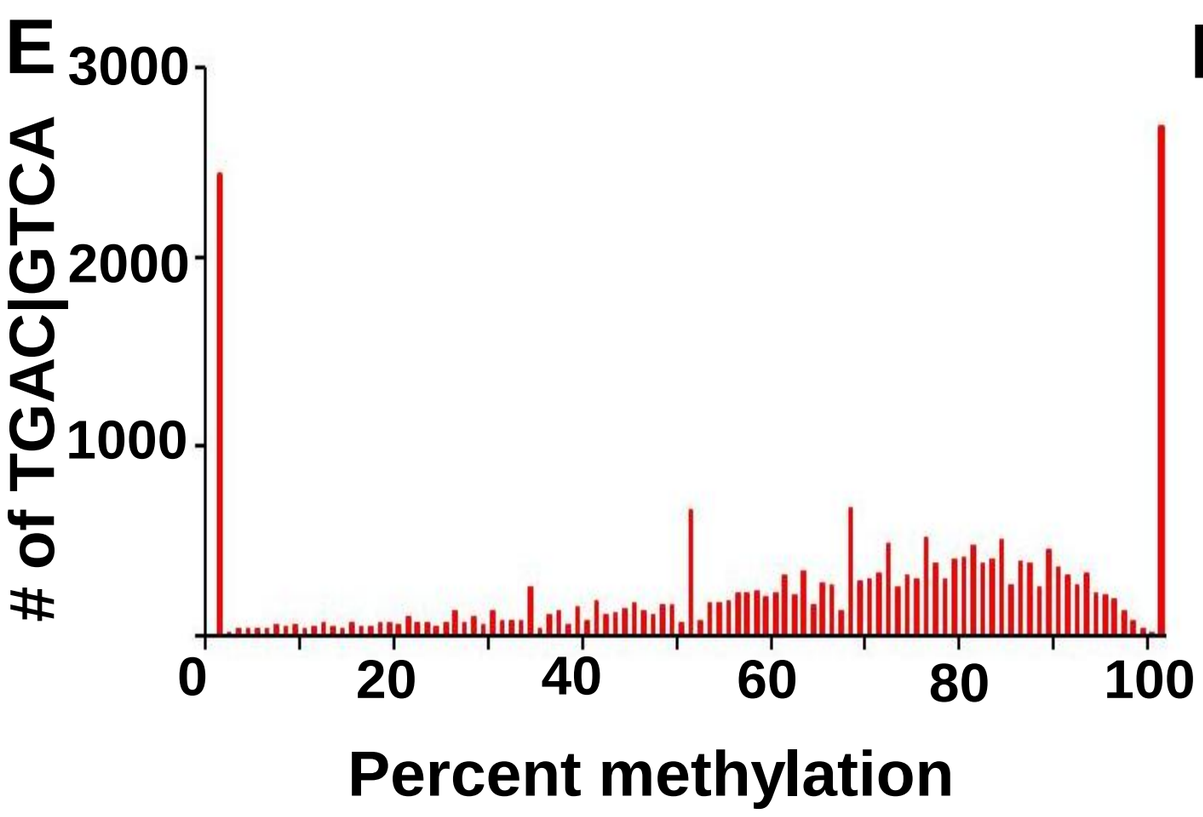

F

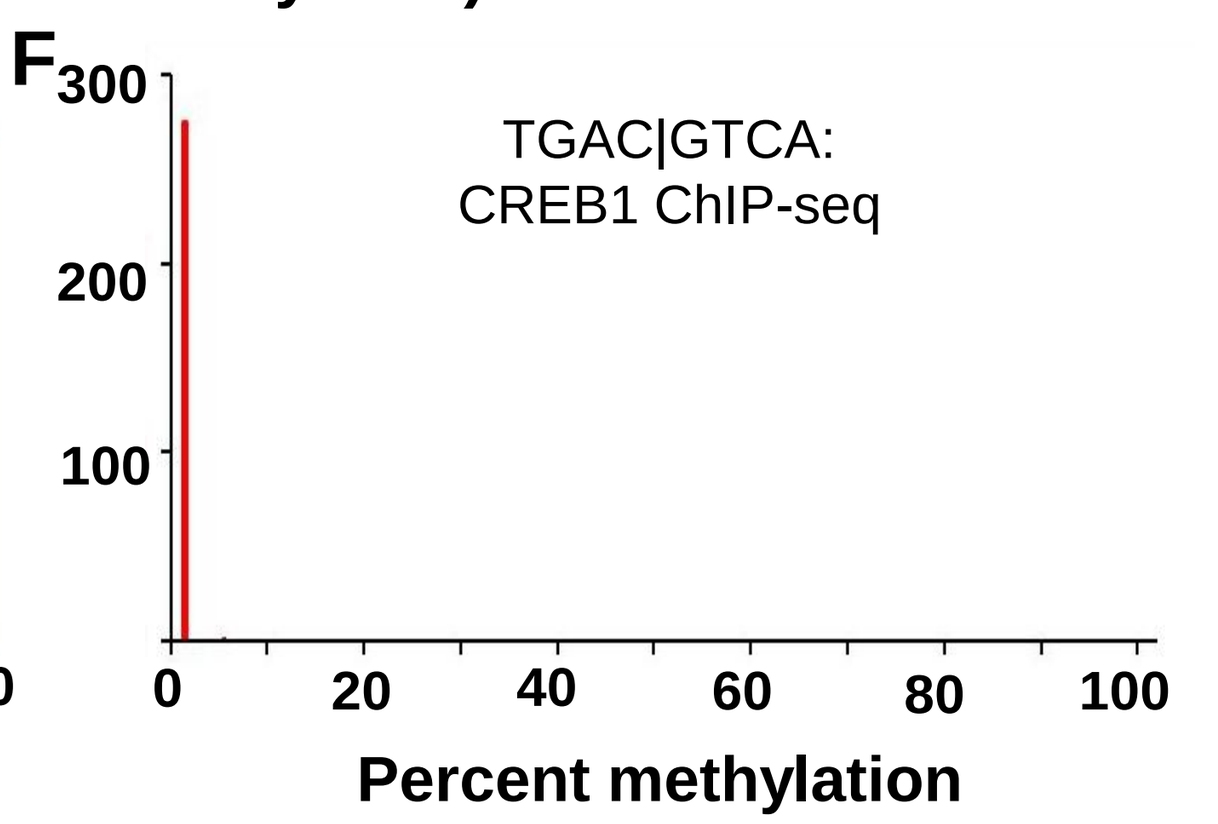

Supplementary Figure 12:

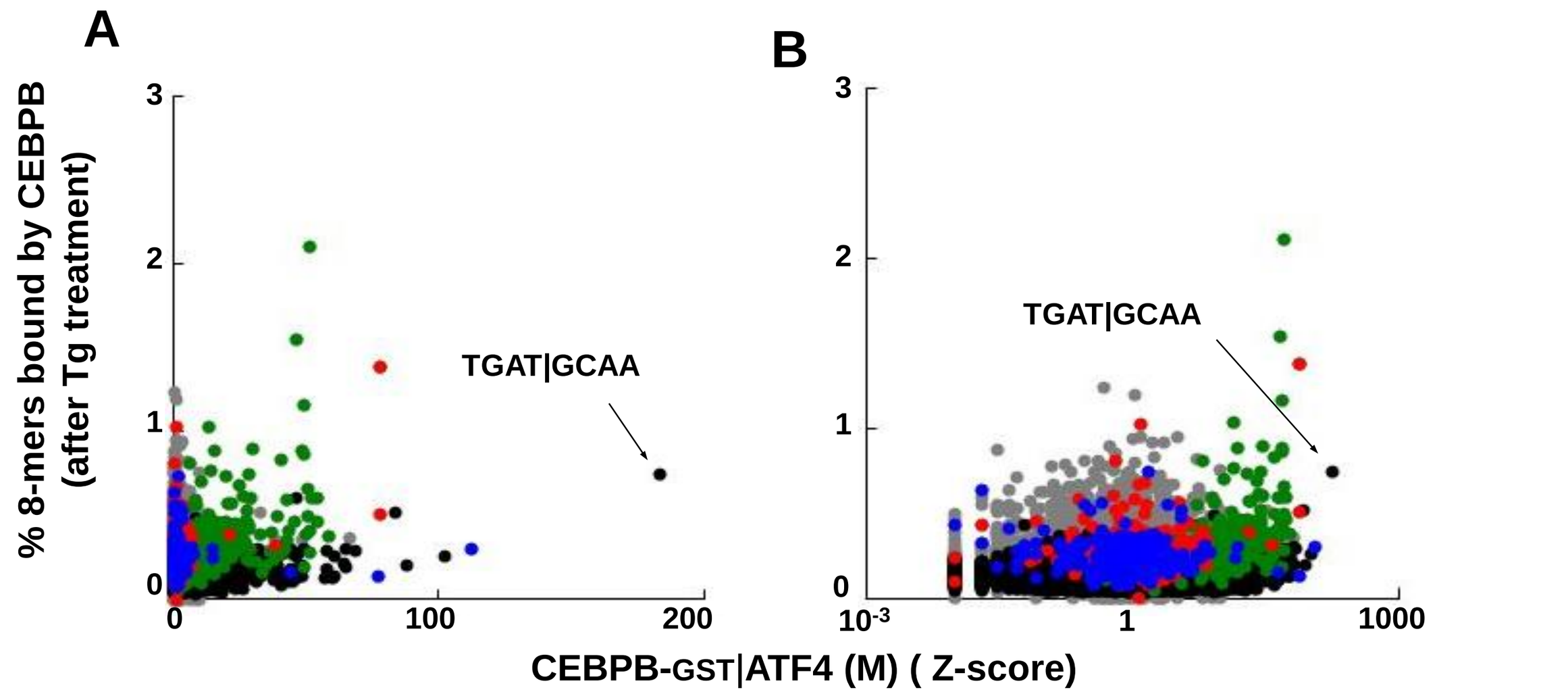

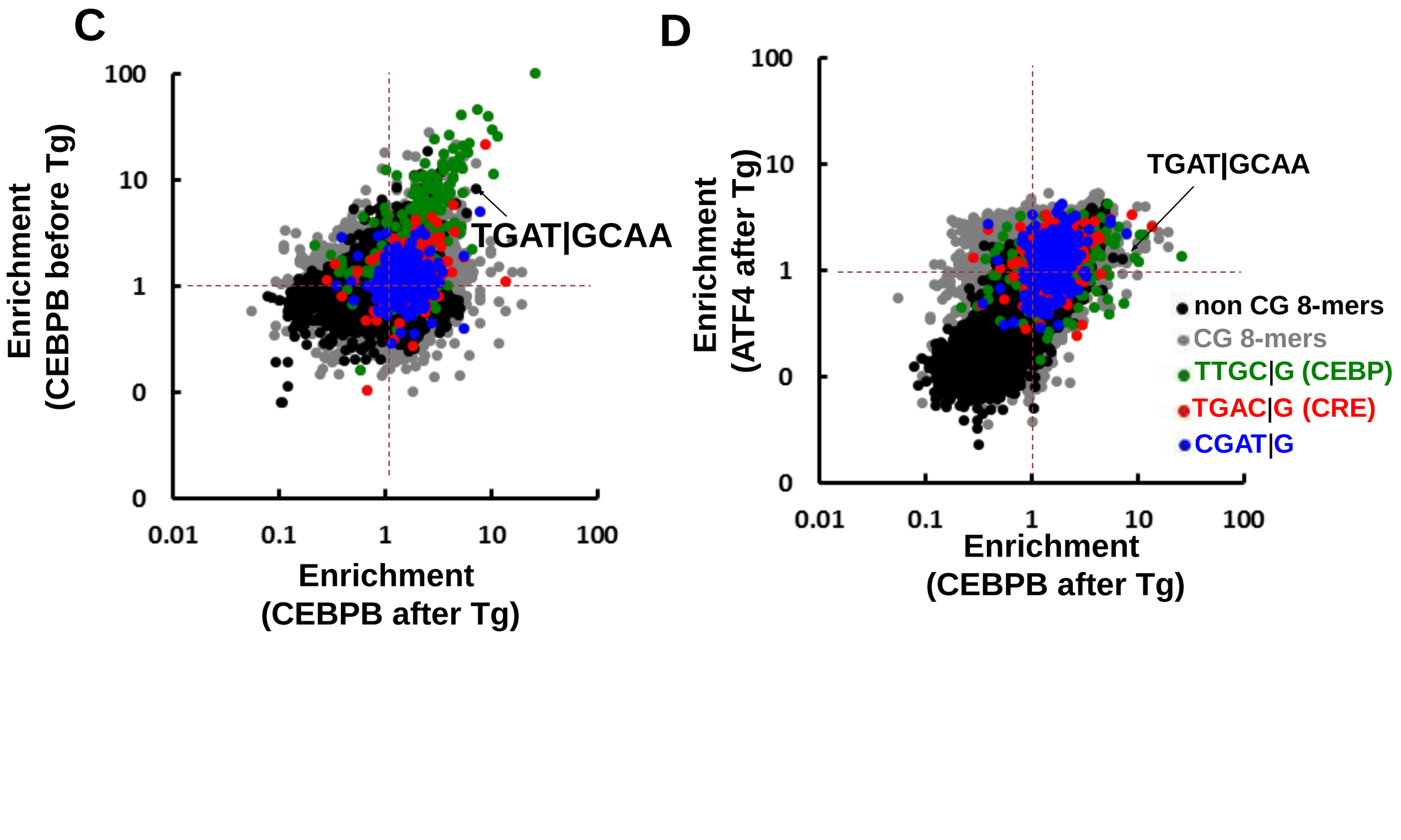

Supplementary Figure 13:

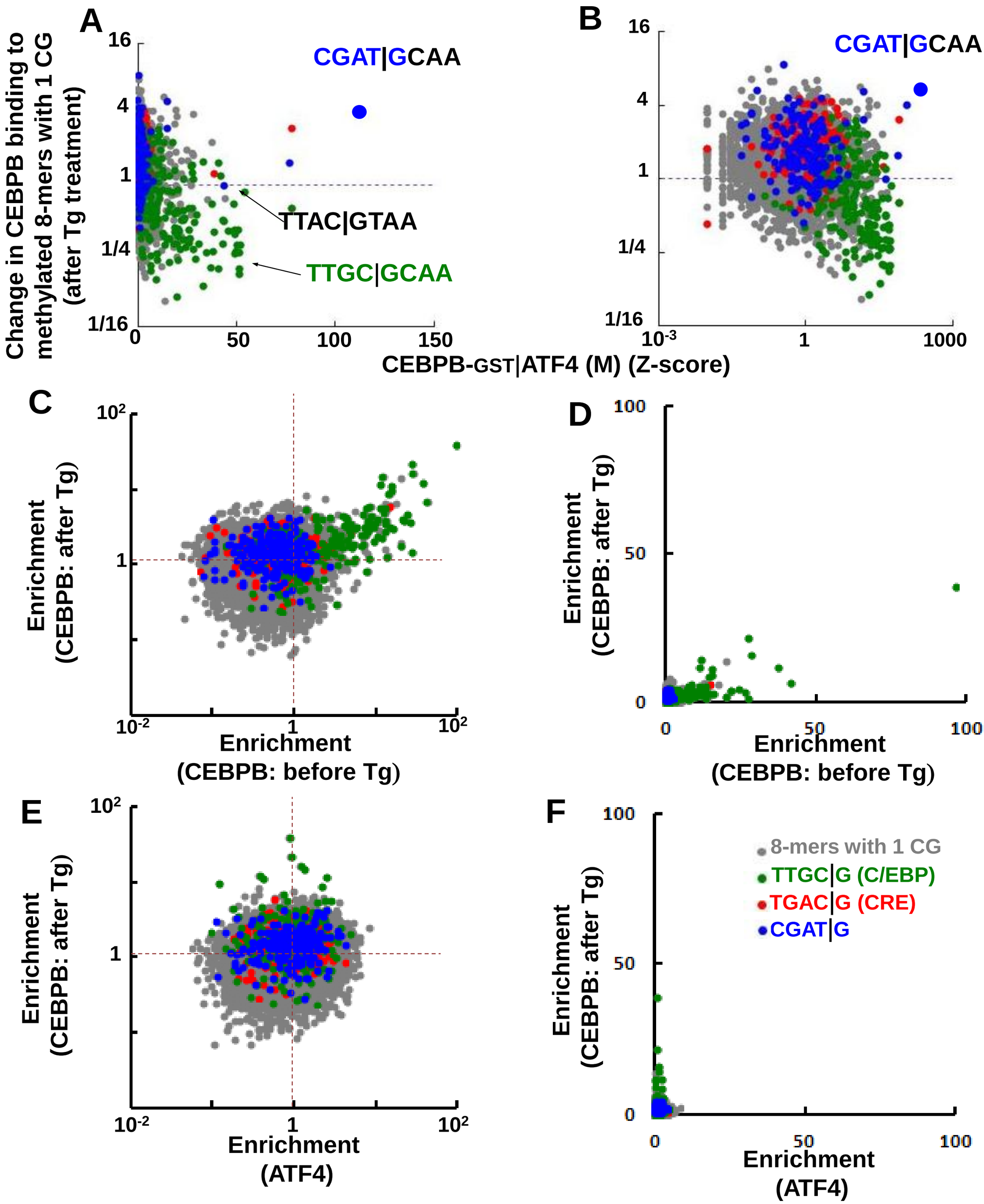

Supplementary Table1A. Estimation of length of CEBP motif (40K array)

	CEBPB		CEBPA		CEBPG		CEBPD	
	UM*	M‡	UM	M	UM	M	UM	M
TGC|GCAAT	70	129	42	84	51	69	26	39
TGC|GCAAG	13	28	12	16	8	15	7	5
TGC|GCAAC	20	33	14	24	16	27	9	10
TGC|GCAAA	5	14	3	6	3	6	2	4

Supplementary Table1B. Estimation of length of CEBP motif (180K array)

	CEBPB		CEBPA	
	UM*	M‡	UM	M
TGC|GCAAT	21.0	25.7	4.4	6.0
TGC|GCAAG	14.3	10.2	2.7	4.5
TGC|GCAAC	14.9	21.2	4.9	5.9
TGC|GCAAA	4.7	7.8	1.3	1.8

Supplementary Table1C. Estimation of length of TRE and CRE motifs (40K array)

	JUN		JUND		ATF4		CREB1	
	UM*	M‡	UM	M	UM	M	UM	M
TGAG TCAT	12	11	28	30	1	1	1	8
TGAG TCAG	4	3	9	5	1	0	0	2
TGAG TCAC	9	9	17	21	1	1	2	9
TGAG TCAA	2	1	3	3	0	0	-1	1
TGAC TCAT	13	15	27	24	1	1	1	7
TGAC TCAG	2	5	8	7	0	-1	-1	1
TGAC TCAC	7	4	15	15	1	1	1	6
TGAC TCAA	2	3	5	4	1	0	1	4
GAC|GTCAT	4	0	6	2	3	0	33	20
GAC|GTCAG	1	1	1	2	3	2	33	15
GAC|GTCAC	2	2	3	2	2	1	32	26
GAC|GTCAA	1	0	2	2	0	1	13	7

*UM, Unmethylated; ‡M, methylated

Supplementary Table1D. P-values for 8-mers (40K and 180K arrays)

Fig [1]	8mer[2]	Score type[3]	Score_Met[4]	Score_Met_Adjusted[5]	Score_UnMet[6]	Diff[7]	Direction [8]	Pval[9]	TF(s)[10]	"DNA binding following CG methylation was…"[11]
1C	TTGCGCAA	Zscores	1286.52	592.83	506.63	86.20	Met_Hi	3.23E-02	CEBPA	enhanced
1D	TTGCGCAA	Zscores	953.23	599.01	583.88	15.13	Met_Hi	1.83E-02	CEBPB	enhanced
1E	TTGCGCAA	Zscores	253.27	272.06	290.84	-18.78	UnMet_Hi	2.20E-03	CEBPD	inhibited
1F	TGACGTCA	Zscores	54.60	38.35	187.10	-148.75	UnMet_Hi	2.11E-28	CREB1	inhibited
1G	TGACGTCA	Zscores	2.47	1.61	13.86	-12.25	UnMet_Hi	1.02E-76	ATF4	inhibited
1H	CGATGCAA	Zscores	112.03	113.10	22.92	90.17	Met_Hi	1.35E-88	CEBPB -GST|ATF4	enhanced
1H	TGACGCAA	Zscores	77.95	78.69	160.58	-81.89	UnMet_Hi	5.35E-96	CEBPB -GST|ATF4	inhibited
S2A	TGACGTCA	Zscores	2.87	2.05	23.75	-21.71	UnMet_Hi	8.72E-84	JUN	inhibited
S2B	TGACGTCA	Zscores	4.05	2.86	30.52	-27.66	UnMet_Hi	7.07E-81	JUND	inhibited
S2C	TTGCGCAA	Zscores	224.86	241.65	273.65	-31.99	UnMet_Hi	1.19E-03	CEBPG	inhibited
3C*	CTGACGCA	Medians	12513.67	7777.64	10012.00	-2234.36	Homo_Hi*	4.68E-03	CEBPB -GST|ATF4 vs CEBPB -GST (UnMet)*	inhibited (hetero)*
3D*	CCGATGCA	Medians	12048.00	7796.14	1295.33	6500.81	Hetero_Hi*	5.01E-03	CEBPB -GST|ATF4 vs C/EBPb-GST (Met)*	enhanced (hetero)*
3D*	ATGACGCA	Medians	9376.50	6083.14	21990.50	-15907.36	Homo_Hi*	6.26E-29	CEBPB -GST|ATF4 vs CEBPB -GST (Met)*	inhibited (hetero)*
3E	CCGATGCA	Medians	12048.00	12073.81	3864.50	8209.31	Met_Hi	3.97E-26	CEBPB -GST|ATF4	enhanced
3E	ATGACGCA	Medians	9376.50	9394.46	9965.33	-570.87	UnMet_Hi	1.78E-02	CEBPB -GST|ATF4	inhibited
S5A	CGATGCAA	Zscores	22.29	13.42	2.96	10.46	Met_Hi	1.66E-08	ATF4-GST|CEBPB	enhanced
S5A	TGACGCAA	Zscores	3.56	2.15	33.99	-31.84	UnMet_Hi	3.62E-97	ATF4-GST|CEBPB	inhibited
S8A	ACGATGCA	Medians	6603.83	5687.49	650.00	5037.49	Met_Hi	4.69E-11	ATF4-GST|CEBPB	enhanced
S8A	CTGACGCA	Medians	1363.50	1104.14	5447.00	-4342.86	UnMet_Hi	2.93E-15	ATF4-GST|CEBPB	inhibited

1 Figure in which the comparison is illustrated.

2 8mer being compared.

3 Type of 8mer score being compared. For 16x arrays, Zscores are used. For 4x arrays, the median signal intensity is used.

4 Raw score on the methylated array.

5 Adjusted score on the methylated array - the score resulting from a linear regression of the methylated scores onto the unmethylated scores (see Methods).

6 Raw score on the unmethylated array.

7 Difference between the adjusted methylated score and the unmethylated score.

8 Direction of the difference (e.g., "Met_Hi" means the 8mer scored higher on the methylated array).

9 P-value of the difference (based on a Z-score transformation comparing to the expected mean and standard deviation of top-scoring 8mers on replicate unmethylated arrays - see Methods)

10 TF(s) tested on the array.

11 "Final verdict", based on the p-value.

*comparison here is between a hetero and homo-dimeric complexes, instead of methylated vs unmethylated arrays

Supplementary Table2: Z-score from 40K array for homodimers (CEBPB and ATF4) and heterodimers (CEBPB-GST|ATF4 and CEBPB|ATF4-GST) for canonical C/EBP, CRE, chimera and CGAT|G site

		CEBPB-GST		ATF4-GST		CEBPB-GST|ATF4		ATF4-GST|CEBPB	
		UM*	M‡	UM	M	UM	M	UM	M
C/EBP	TTGC|GCAA	584	953	3	2	69	52	1	2
CRE	TGAC|GTCA	7	8	14	2	34	21	15	3
CGATG	CGAT|GCAA	4	4	1	0	23	112	3	22
Chimera	TGAC|GCAA	86	119	3	3	161	78	34	4
Chimera-1	TGAT|GCAA	47	45	1	2	178	183	39	26
worst	NNNNNNNN	-4	-3	-4	-3	-3	-3	-4	-3

*UM, Unmethylated; ‡M, methylated

Supplementary Table 3A: Ratio of fluorescence intensities for the best versus the worst bound 8-mers from 180K array

	CEBPA-GST		CEBPB-GST		ATF4-GST		CEBPB-GST|ATF4		ATF4-GST|CEBPB	
	UM*	M‡	UM*	M‡	UM	M	UM	M	UM	M
Ratio: best/ worst	45	44	267	191	22	16	181.4	156.1	126.2	71.8

Supplementary Table 3B: Fluorescence intensities (×1,000) from 180K array for homodimers (CEBPB and ATF4) and heterodimers (CEBPB-GST|ATF4 and CEBPB|ATF4-GST) for canonical CEBP, CRE, chimera and CGATG site

		CEBPB-GST		ATF4-GST		CEBPB-GST|ATF4		ATF4-GST|CEBPB	
		UM*	M‡	UM	M	UM	M	UM	M
C/EBP	ATTGC|GCAA	22.8	30.6	1.5	2.2	3.7	4.2	0.6	0.7
CRE	ATGAC|GTCA	2.5	4.6	13.8	2.4	1.8	2.6	9.3	1.7
CGATG	CCGAT|GCAA	0.8	1.3	1.3	1.9	3.9	12	1.1	11
Chimera	CTGAC|GCAA	10.0	13.2	1.8	1.8	12.5	8.2	12.9	3.4
Chimera-1	CTGAT|GCAA	8.4	8.9	1.9	2.1	15.8	13.8	13.1	14.6
worst	NNNNNNNNA	0.1	0.2	0.6	0.6	0.1	0.1	0.1	0.2

Supplementary Table 3C: Methylated 8-mer NCGAT|GCA*A* bound well by CEBPB|ATF4 heterodimer: fluorescence intensity (X1000) from 180K array

	CEBPB-GST		ATF4-GST		CEBPB-GST|ATF4		ATF4-GST|CEBPB	
	UM*	M‡	UM	M	UM	M	UM	M
CCGAT|GCAA	0.8	1.3	1.3	1.9	3.9	12	1.1	11
ACGAT|GCAA	0.9	1.9	1.3	1.8	3	11.6	1.3	13.1
GCGAT|GCAA	0.8	1.8	1.6	2.4	3.3	10.6	1.2	10.4
TCGAT|GCAA	0.7	1	1.8	1.7	2.2	5.9	1.4	4.6

*UM, Unmethylated; ‡M, methylated

Supplementary Table 4A. Genome wide cytosine methylation of mouse primary dermal fibroblasts

	CT strand			GA strand		
	Total	Unmethylated	Methylated	Total	Unmethylated	Methylated
CpG	20,198,742	5,120,127 (25.35%)	15,078,615 (74.65%)	20,200,725	5,119,883 (25.35%)	15,080,842 (74.65%)
CHG	104,729,135	104,668,326 (99.94%)	60,809 (0.06%)	104,720,502	104,662,171 (99.94%)	58,331 (0.06%)
CHH	353,973,395	353,791,950 (99.95%)	181,445 (0.05%)	354,056,680	353,876,705 (99.95%)	179,975 (0.05%)

Supplementary Table4B. Genome-wide methylation and CEBPB binding for certain sequences

ATF4		Motifs	# Motifs in Genome	# with methylation coverage	Unmethylated motifs	Methylated motifs	Bound by CEBPB
					(% bound by CEBPB)	(% bound by CEBPB)	(% Methylated)
	10-mer	ATTGC|GCAAT	119	115	12 (83%)	103 (35%)	45 (80%)
	8-mer	TTGC|GCAA	2,119	1,999	220 (54%)	1,779 (11%)	306 (61%)
-	8-mer	TTGT|GCAA	81,910	-	81,910 (1.7%)		1,413
	7-mer	CGAT|GCA*	29,611	28,384	4,323 (1.0%)	24,061 (0.1%)	59 (24%)
	8-mer	TGAT|GCAA*	48148	-	48,148 (0.7%)	-	351
	10-mer	ATTGC|GCAAT	119	115	12 (0.0%)	103 (9.7%)	10 (100%)
	8-mer	TTGC|GCAA	2,119	1,999	220 (1.4%)	1,779 (2.3%)	44 (93%)
+	8-mer	TTGT|GCAA	81,910	--	81,910 (0.2%)	--	136
	7-mer	CGAT|GCA*	29,611	28,384	4,323 (0.4%)	24,061 (0.1%)	46 (61%)
	8-mer	TGAT|GCAA*	48,148	--	48,148 (0.5%)	--	264

Supplementary Table 4C. CREB1 binding to unmethylated and methylated CRE 8-mers (TGAC|GTCA) in mouse primary dermal fibroblasts

TGAC|GTCA	Unmethylated	Methylated	Total
CREB1 Bound	141	0	141
CREB1 not Bound	4,691	9,465	14,156
Total	4,832	9,465	14,297

Supplementary Table 5A. *In vivo* and *in vitro* CEBPB binding to unmethylated and methylated C/EBP like 9-mers

9-mers	# 9-mers in Genome	# 9-mers with methylation coverage	Unmethylated 9-mers				Methylated 9-mers			
			In vitro ($x10^3$)	Ratio	# (% bound)	Ratio	In vitro ($x10^3$)	Ratio	# (% bound)	Ratio
TTGC|GCAAT	479	446	21	1	46 (74%)	1	25	1	400 (17.5%)	1
TTGC|GCAAC	370	354	14.9	0.71	52 (63%)	0.85	21.2	0.85	302 (17.8%)	1.02
TTGC|GCAAG	597	574	14.3	0.68	64 (47%)	0.64	10.2	0.41	510 (8.6%)	0.49
TTGC|GCAAA	674	625	4.7	0.22	51 (41%)	0.55	7.8	0.31	574 (3.5%)	0.20

Supplementary Table 5B. CEBPB binding to unmethylated and methylated C/EBP like 10-mers in mouse primary dermal fibroblasts

Motifs	# in Genome	# in Peak	%bound	Masked Genome			
				# in Genome	# with methylation coverage	Unmethylated (CEBPB binding)	Methylated (CEBPB binding)
ATTGC|GCAAT	119	45	38%	101	98	11(82%)	87(39%)
ATTGC|GCAAC	170	55	32%	127	125	17(82%)	108(28%)
GTTGC|GCAAC	76	27	36%	46	45	12(75%)	33(27%)
ATTGC|GCAAG	255	46	18%	164	163	30(63%)	133(17%)
CTTGC|GCAAC	210	45	21%	141	138	29(66%)	109(16%)
CTTGC|GCAAG	205	25	12%	143	142	24(46%)	118(8%)
ATTGC|GCAAA	316	33	10%	244	236	28(46%)	208(8%)
GTTGC|GCAAA	221	17	8%	153	148	22(36%)	126(5%)
CTTGC|GCAAA	353	16	5%	268	262	34(21%)	228(3%)
TTTGC|GCAAA	195	4	2%	150	139	15(7%)	124(2%)

Supplementary Table 6A. Enriched GO Terms for CEBPB bound genes with TGAT|GCAA motifs after ATF4 induction by thapsigargin

	Term		Count	P-Value	Fold Enrichment
TGAT|GCAA	GO:0006418	tRNA aminoacylation for protein translation	3	0.01	19.26
	GO:0043039	tRNA aminoacylation	3	0.01	19.26
	GO:0043038	amino acid activation	3	0.01	19.26

Supplementary Table 6B. P-values based on fraction of CEBP ChIP-seq peaks vs non peaks containing K-mers with mCGAT|G before and after ATF4 induction

Kmers	P-value
mCGAT|GCAA	1.05E-03
mCGAT|GCA	6.52E-06
mCGAT|GC	9.49E-17
mCGAT|GT	2.11E-06
mCGAT|G	2.46E-28

Supplementary Table 6C. Enriched GO Terms for CEBPB bound genes with CGAT|G motifs after ATF4 induction by thapsigargin

CGAT|G	Term		Count	P-Value	Fold Enrichment
Unmethylated	GO:0006915	apoptosis	6	0.048	2.97
Methylated	GO:0006468	protein amino acid phosphorylation	8	0.002	4.36
	GO:0006793	phosphorus metabolic process	9	0.002	3.62
	GO:0006605	protein targeting	3	0.053	7.86

Supplementary Table 7: B-ZIP domain sequences used in this study

C-terminal GST tag	basic region	leucine zipper
ATF4	PYDPPGVSLTAKVKTEKLDKKLKKMEQNKTAATRYRQKKRAEQEALTG	ECKELEKKNEALKEKADSLAKEIQYLKDLIEEVRKARGKKRVP
CREB1	VVMASSPALPTQPAEEAARKREVRLMKNREAARECRRKKKEYVKCLEN	RVAVLENQNKTLIEELKALKDLYCHKSD
JUN	MPGETPPLSPIDMESQERIKAERKRMRNRIAASKCRKRKLERIARLEE	KVKTLKAQNSELASTANMLREQVAQLKQKVMNHVNSGCQLMLTQQLQ
JUND	SFGDSPPLSPIDMDTQERIKAERKRLRNRIAASKCRKRKLERISRLEE	KVKTLKSQNTELASTASLLREQVAQLKQKVLSHVNSGCQLLPQHQVP
CEBPA	GSGAGAGKAKKSVDKNSNEYRVRRERNNIAVRKSRDKAKQRNVETQQ	KVLELTSDNDRLRKRVEQLSRELDTLRGIFRQLPESSWSRPWATA
CEBPB	PPAAPAKAKAKKTVDKLSDEYKMRRERNNIAVRKSRDKAKMRNLETQH	KVLELTAENERLQKKVEQLSRELSTLRNLFKQLPEPLLASAGHC
CEBPD	PGTVREKGAGKRGPDRGSPEYRQRRERNNIAVRKSRDKAKRRNQEMQQ	KLVELSAENEKLHQRVEQLTRDLAGLRQFFKKLPSPPFLPPTGADCR
CEBPG	AVPPSKQSKKSSPMDRNSDEYRQRRERNNMAVKKSRLKSKQKAQDTLQ	RVNQLKEENERLEAKIKLLTKELSVLKDLFLEHAHSLADNVQPISTETTATNSDNPGQ
N-terminal φ10 tag		
ATF4	VAAKVKGEKLDKKLKKMEQNKTAATRYRQKKRAEQEALTG	ECKELEKKNEALKERADSLAKEIQYLKDLIEEVRKARGKKRVP
CEBPB	KAKKTVDKLSDEYKMRRERNNIAVRKSRDKAKMRNLETQH	KVLELTAENERLQKKVEQLSRELSTLRNLFKQLPEPLLASAGHC
Consensus	-BB-BN--AA-B-R-BB------L--	----L------L------L------L------L